

Impregnation Process of Vegetable Fiber Reinforcement for Composites: Multi-Scale Analysis

Chung-Hae PARK

Professor, IMT Nord Europe

chung-hae.park@imt-nord-europe.fr

Composites Manufacturing

Raw materials



Fiber



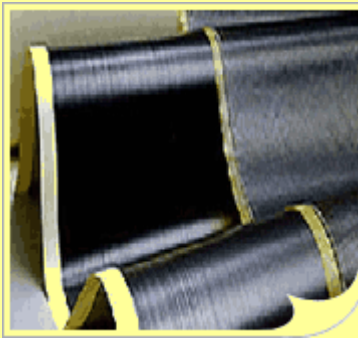
Fabric



Resin

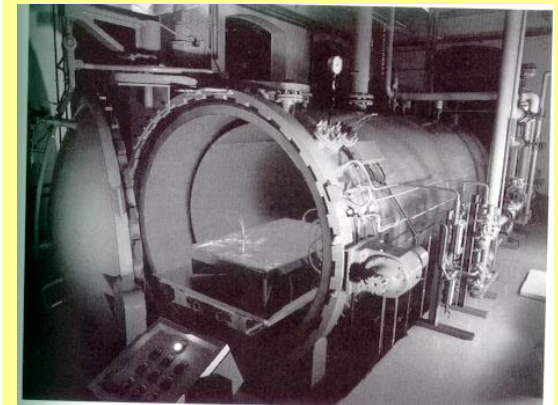
Semi-product

Prepreg



Final product

Autoclave

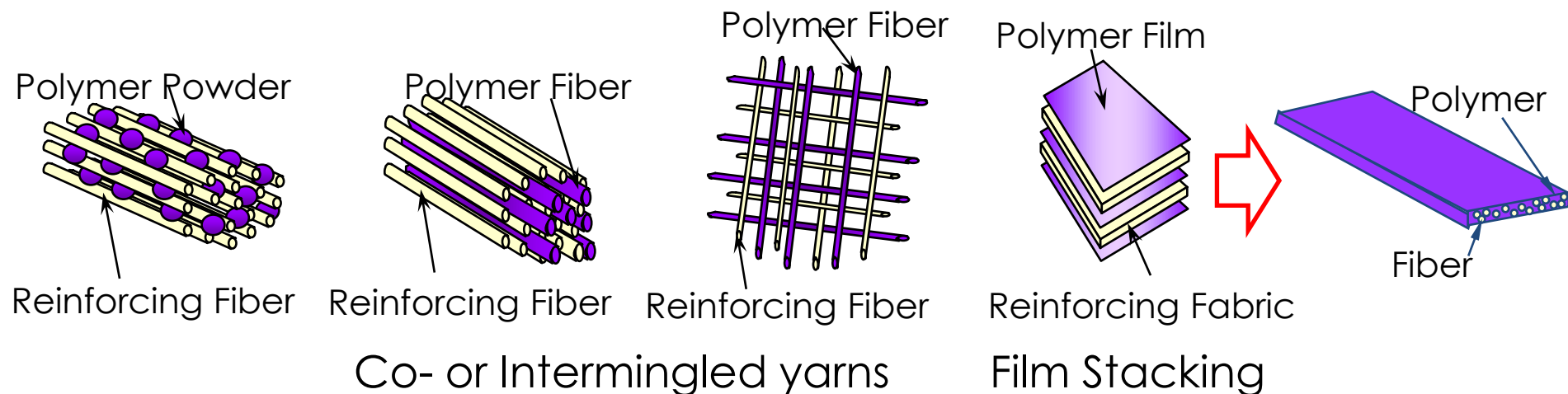


**Direct fabrication
Out of autoclave !**

Impregnation with Thermoplastics

- Resin Impregnation under heat and pressure
 1. Powder Impregnation
 - Powder + Binder + Liquid
 - Adhere Powder using Electrostatics(Atochem)
 2. Co- or Intermingled yarns (resin fiber + reinforcing fiber)
 3. Film Stacking (Resin films + reinforcing fabric)
 4. Direct Impregnation (In-situ polymerization)

*High viscosity of
thermoplastics:
Fiber-matrix
premixed form*

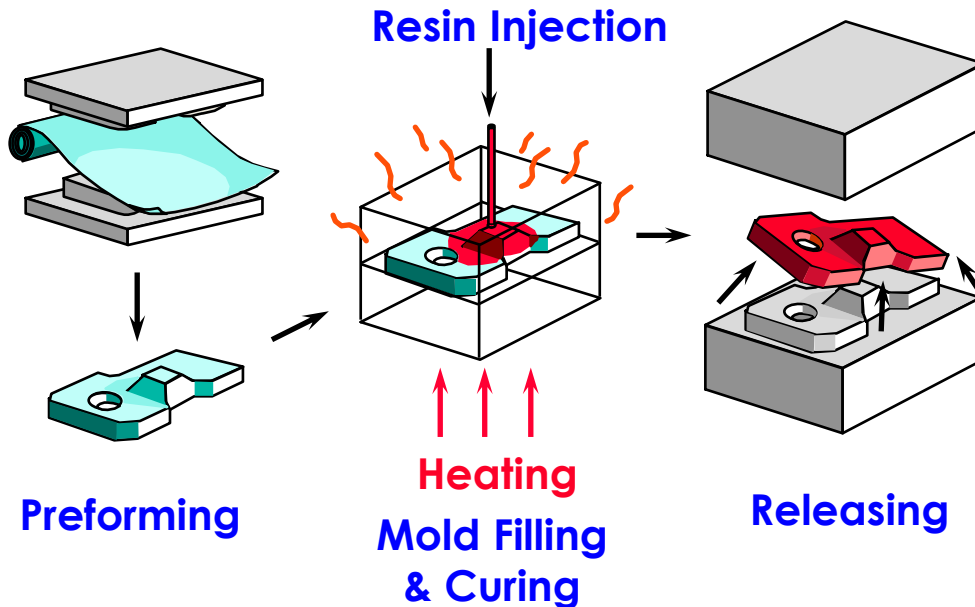


Liquid Composite Molding

Direct impregnation of dry fiber reinforcement by liquid resin

Low viscosity resin: Thermosets (& some Thermoplastics)

■ Resin Transfer Molding process



- ✓ Large and complex structures without assembling
- ✓ Reduction of raw material cost and labor
- ✓ Free from volatile trouble

A320/A340 spoiler
Preform



Final product
Terry Mcgrail, Cytec

Flow Modeling

- **Conservation Laws**

Mass (incompressible fluid)

Momentum (Navier-Stokes eq.)

Energy

$$\nabla \cdot \vec{v} = 0$$

$$\frac{\partial \vec{v}}{\partial t} + \vec{v} \cdot \nabla \vec{v} = -\frac{1}{\rho} \nabla P + \nu \nabla^2 \vec{v} + \vec{g}$$

$$\rho C_p \frac{DT}{Dt} = k \nabla^2 T + \frac{1}{2} \mu (\dot{\gamma} : \dot{\gamma})$$

- **Constitutive Relations**

Darcy's law

Non-newtonian relation

Viscoelastic relation

Viscous heat dissipation
(Very important for thermoplastic injection molding)

- **Boundary Conditions**

Problems :

① *What to neglect*

② *Boundary conditions*

③ *Efficient analysis method*

Requires physical insights, experiences, some preliminary experiments, etc.

Darcy's Law & Mass Conservation

- **Flow through Porous Medium** (low Re : Creeping flow, Stokes flow)

$$\frac{Q}{A} = V = (1 - v_f) V_{pore} = -\frac{K}{\mu_r} \nabla p$$

V : Darcy velocity (volume averaged velocity)

V_{pore} : Pore velocity (actual resin advancing velocity)

K : Permeability (Hydraulic conductivity of porous medium)

μ_r : Fluid viscosity

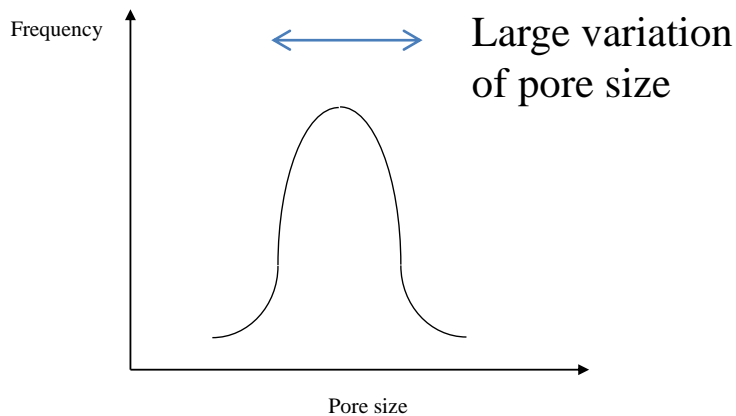
- **Mass conservation of incompressible fluid**

$$-\nabla \cdot \vec{V} = 0; \quad \nabla \left(\frac{K}{\mu_r} \nabla p \right) = 0$$

- ✓ Only one unknown (pressure): no momentum equation required.
- ✓ Quasi-steady state; new pressure field with moving boundary at each instant

Single Scale Porous Medium: Mat

■ Pore size distribution

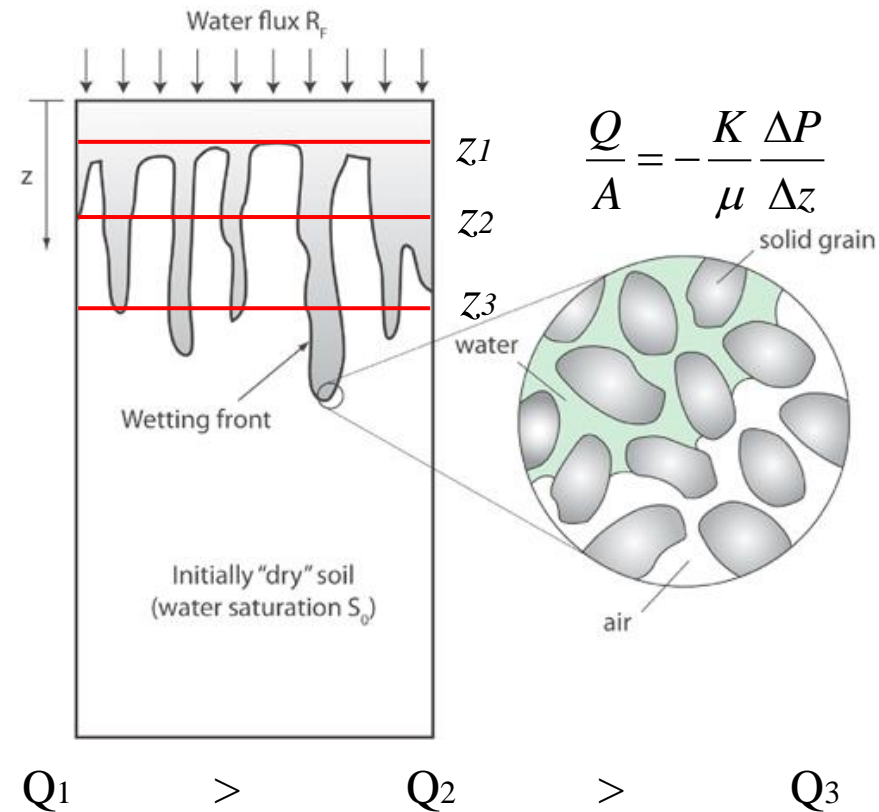


Sand stone



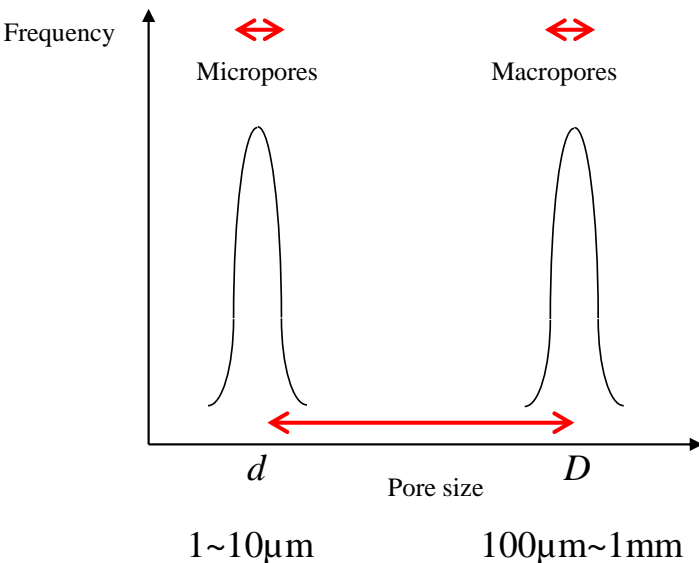
Chopped strand mat

■ « Fingering »

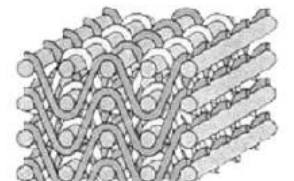
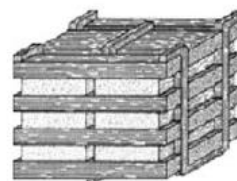
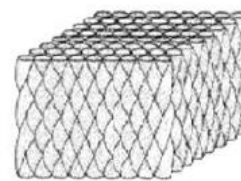
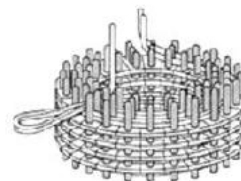
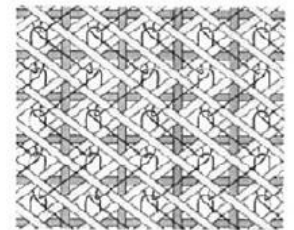
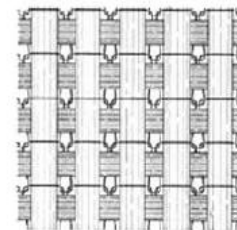
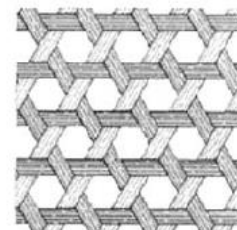
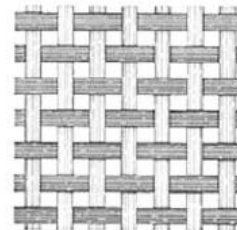
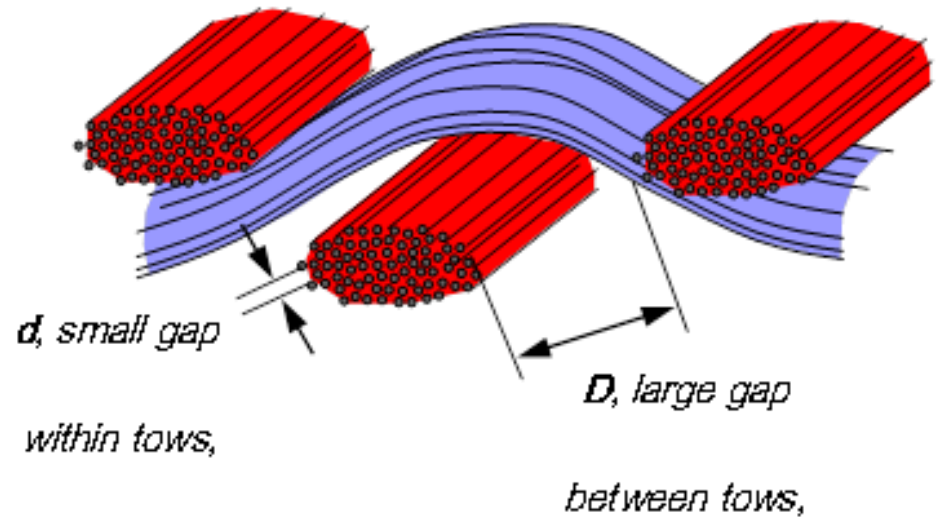


Double Scale Porous Medium: Textile

■ Pore size distribution



- Big difference in pore size between two groups
- Narrow variation of pore size in each group



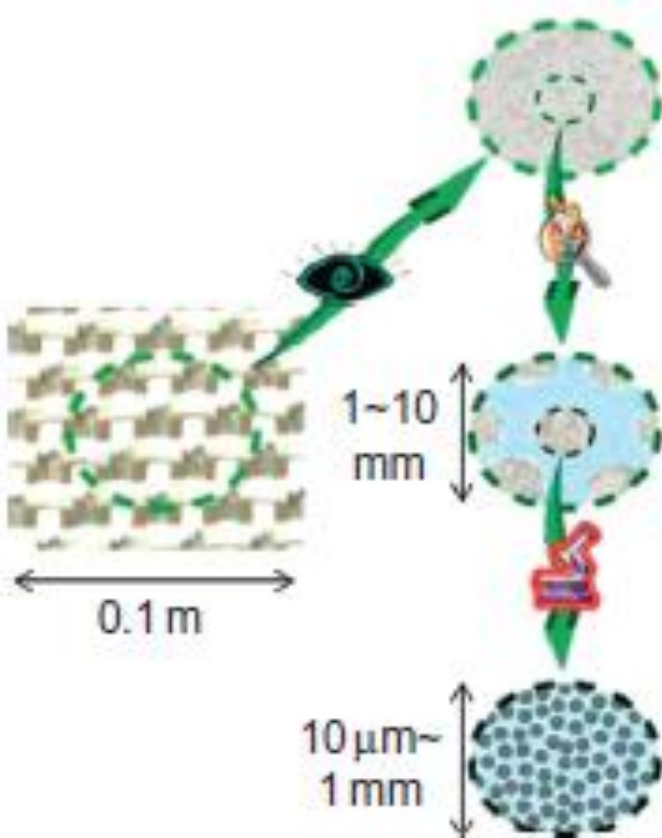
3-D Cylindrical Construction

3-D Braiding

3-D Orthogonal Fabric

Angle-Interlock Construction

Resin Flow Models vs. Scale



MACRO: Homogeneous porous medium

Darcy's law $\bar{u} = -\frac{\tilde{K}_{\text{preform}}}{\mu} \nabla P$

MESO: Open gap and porous medium

Stokes flow $-\nabla P + \mu \nabla^2 \bar{u} = 0$

$$P_{\text{cap}} = \frac{4 \sigma \cos \theta}{D_{\text{pore}}}$$

Darcy's law with capillary pressure

$$\bar{u} = -\frac{\tilde{K}_{\text{tow}}}{\mu} \nabla (P - P_{\text{cap}})$$

MICRO: Solid filaments and tiny pore

$$\vec{f}_s = \sigma \kappa \vec{n} \delta_s$$

Stokes flow with surface tension

$$-\nabla P + \mu \nabla^2 \bar{u} + \vec{f}_s = 0$$

■ Stokes-Brinkman equation

$$\rho \left[\frac{\partial \vec{u}}{\partial t} + \vec{u} \cdot \nabla \vec{u} \right] = -\nabla P - \frac{\mu}{\tilde{K}} \vec{u} + \mu_e \nabla^2 \vec{u} + \vec{f}_b$$

✓ **Macropore** $\tilde{K} = \infty, \mu_e = \mu$

$$0 = -\nabla P + \mu \nabla^2 \vec{u} + \vec{f}_b$$

Stokes

✓ **Micropore** $\mu_e = 0, P = P_{\text{cap}}$ at resin-air interface

$$0 = -\nabla P - \frac{\mu}{\tilde{K}} \vec{u}$$

Darcy

Permeability & Compressibility

In general, fabric properties are expressed in terms of **fiber volume fraction**.

- Fiber stress (Compressibility)

$$\sigma_s = A_s \frac{\sqrt{\frac{V_f}{V_{f,0}}} - 1}{\left(\sqrt{\frac{V_f}{V_{f,0}}} - 1 \right)^4}$$

Gutowski

$$\sigma_s = c(V_f)^d$$

Toll and Manson

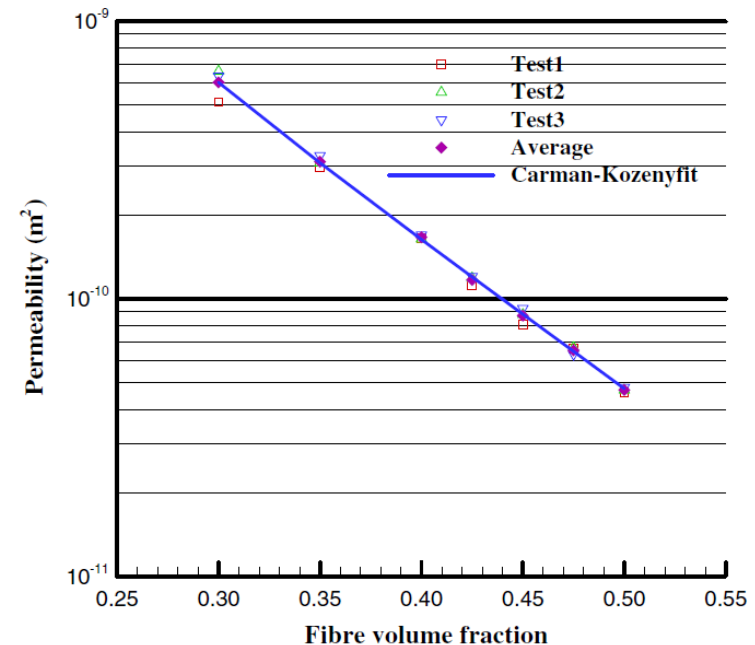
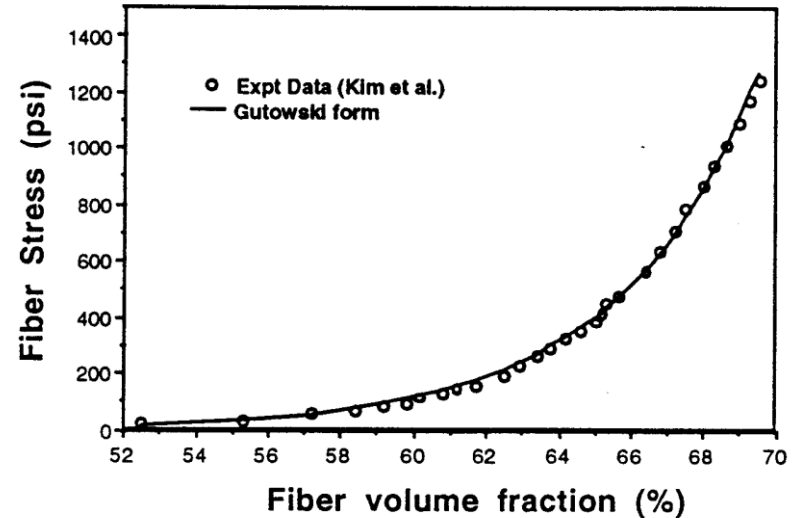
- Permeability

$$K_{ij} = \frac{d_f^2}{16\kappa_{ij}} \frac{(1-V_f)^3}{V_f^2}$$

Kozeny-Carman

$$K_{ij} = a(V_f)^b$$

Power law

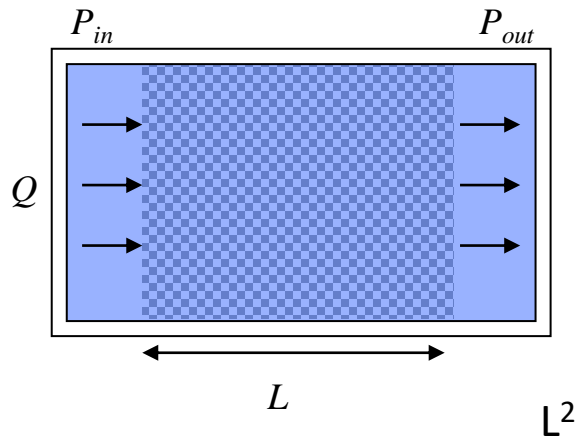


Permeability Measurement

■ Saturated permeability

Constant flow rate

Measure pressure gradient

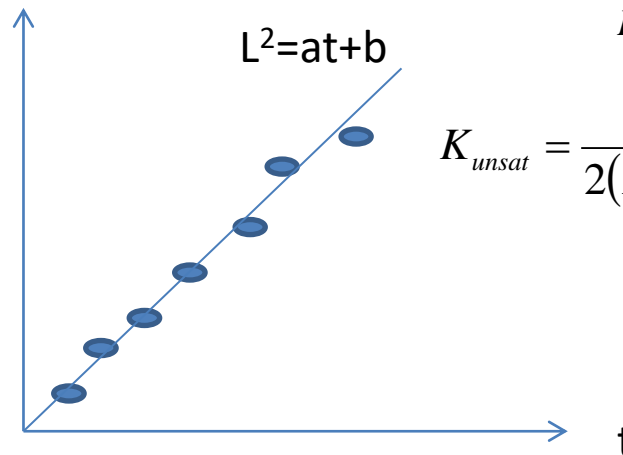
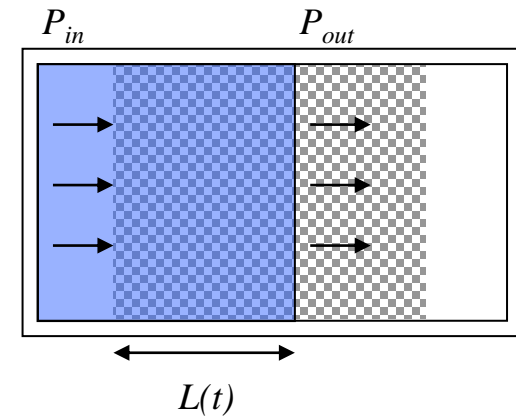


$$K_{sat} = \frac{Q}{A} \frac{\mu L}{P_{in} - P_{out}}$$

■ Unsaturated permeability

Constant pressure drop

Measure flow front progress

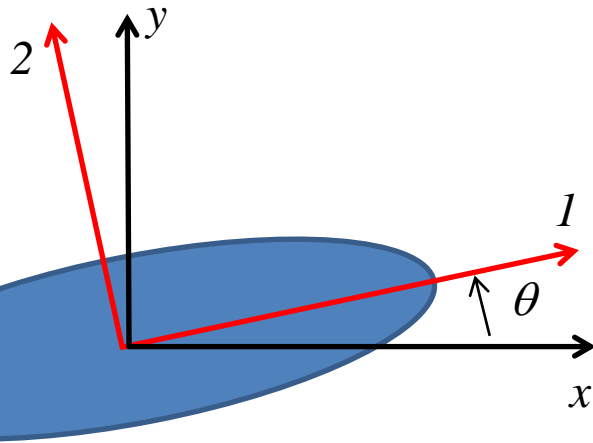


$$K_{unsat} = \frac{\phi \mu L^2}{2(P_{in} - P_{out})t}$$

By curve-fitting

Permeability Tensor

Global permeabilities



$$\begin{bmatrix} K_{xx} & K_{xy} & K_{xz} \\ K_{yx} & K_{yy} & K_{yz} \\ K_{zx} & K_{zy} & K_{zz} \end{bmatrix} = [T_z][T_y][T_x] \begin{bmatrix} K_1 & 0 & 0 \\ 0 & K_2 & 0 \\ 0 & 0 & K_3 \end{bmatrix} [T_x]^{-1} [T_y]^{-1} [T_z]^{-1}$$

Principal permeabilities

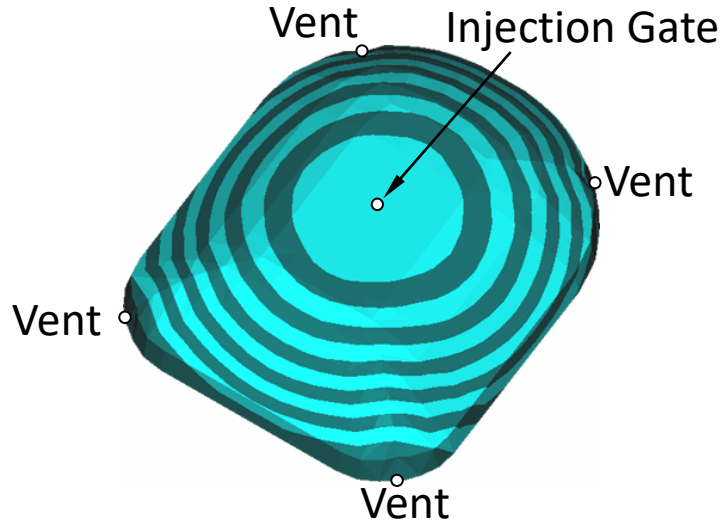
$$[T_x] = \begin{bmatrix} 1 & 0 & 0 \\ 0 & \cos \theta_x & -\sin \theta_x \\ 0 & \sin \theta_x & \cos \theta_x \end{bmatrix}, \quad [T_y] = \begin{bmatrix} \cos \theta_y & 0 & \sin \theta_y \\ 0 & 1 & 0 \\ -\sin \theta_y & 0 & \cos \theta_y \end{bmatrix}, \quad [T_z] = \begin{bmatrix} \cos \theta_z & -\sin \theta_z & 0 \\ \sin \theta_z & \cos \theta_z & 0 \\ 0 & 0 & 1 \end{bmatrix}$$

2D

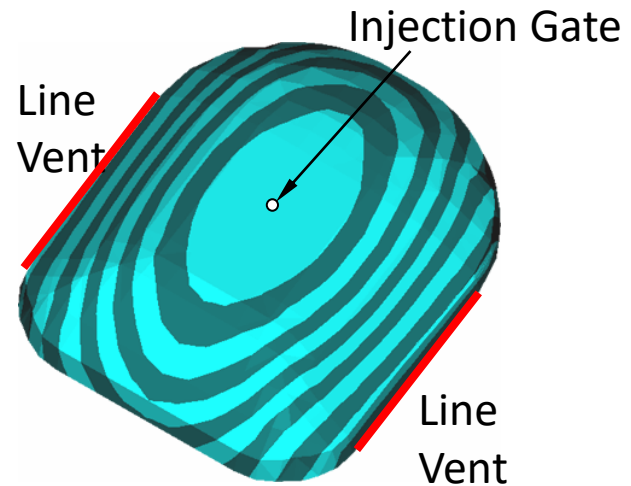
$$\begin{bmatrix} K_{xx} & K_{xy} \\ K_{yx} & K_{yy} \end{bmatrix} = \begin{bmatrix} K_1 \cos^2 \theta + K_2 \sin^2 \theta & (-K_1 + K_2) \sin \theta \cos \theta \\ (-K_1 + K_2) \sin \theta \cos \theta & K_1 \sin^2 \theta + K_2 \cos^2 \theta \end{bmatrix}$$

Anisotropic Permeability

- Anisotropic Permeability Affects the Resin Flow Pattern

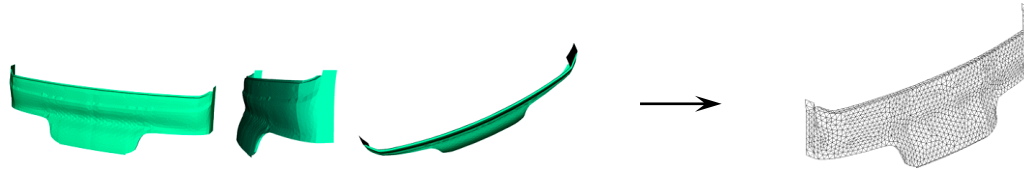


Isotropic ($K_{xx}/K_{yy}=1$)

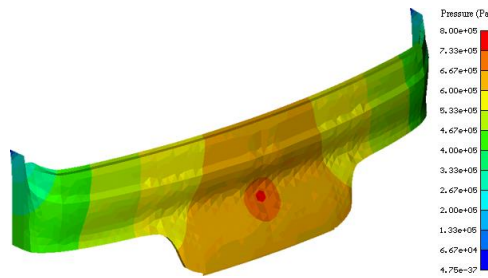


Anisotropic ($K_{xx}/K_{yy}=0.25$)

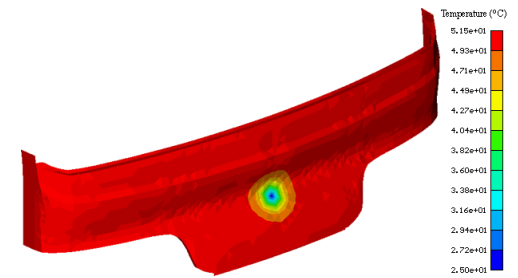
FEM Simulation Example



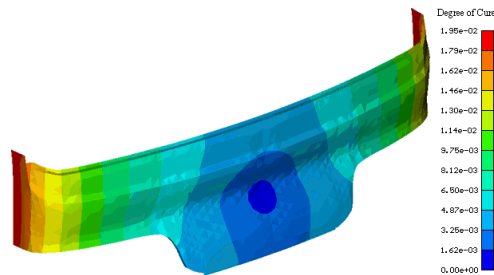
Mold Filling Pattern



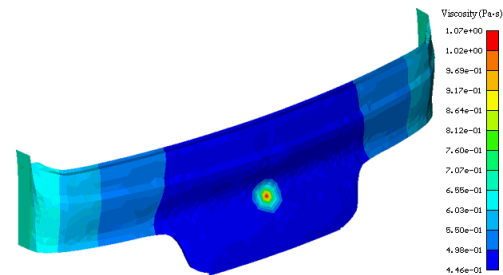
Pressure



Temperature



Degree of Cure



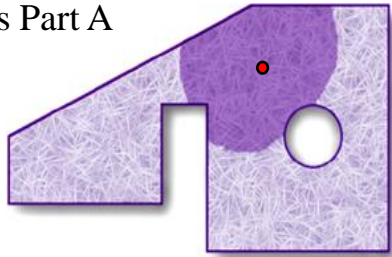
Viscosity

Resin Injection Strategies

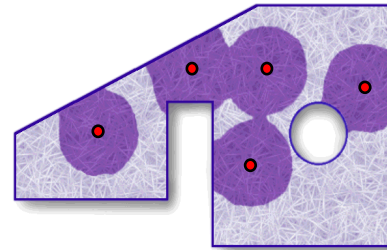
$$\vec{u} = -\frac{K}{\mu} \nabla P = -\frac{K}{\mu} \frac{P}{\Delta x}$$

$$\vec{u} \uparrow \begin{cases} K \uparrow & \text{Fiber Volume Fraction} \downarrow \\ \mu \downarrow & \text{Temperature} \uparrow \\ P \uparrow \\ \Delta x \downarrow & \text{Number of Injection Gates} \uparrow \end{cases}$$

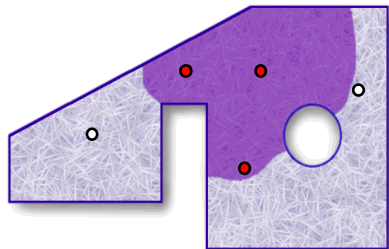
Kang et al., Composites Part A
31 (2000) 407-422



Single Gate Injection
(*Slow Filling*)

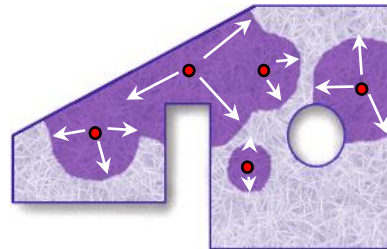


Simultaneously Opened Multiple Gates
(*Many Vents*)



- Open Gates
- Closed Gates

Progressively Opened Multiple Gates
(*Fast Filling*)



Multiple Gates with Variable Injection Pressure
(*Faster Filling*)

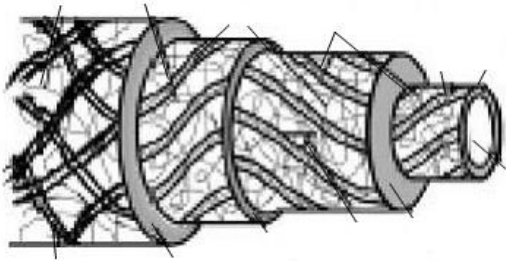
Vegetable Fibers for Composites

Biofiber composites are 10~20 % lighter than glass fiber composites.



Fig. 9. Lignocellulosic reinforcements. (a) Banana; (b) sugarcane bagasse; (c) curauá; (d) flax; (e) hemp; (f) jute; (g) sisal; (h) kenaf. Typical pattern of reinforcements used in the hybrid LC based biodegradable composite synthesis. (i) Jute fabric; (j) ramie-cotton fabric, (k) jute-cotton fabric. (j—reproduced with the kind permission of the Editor [169]).

Flax Fiber, Yarn & Fabric



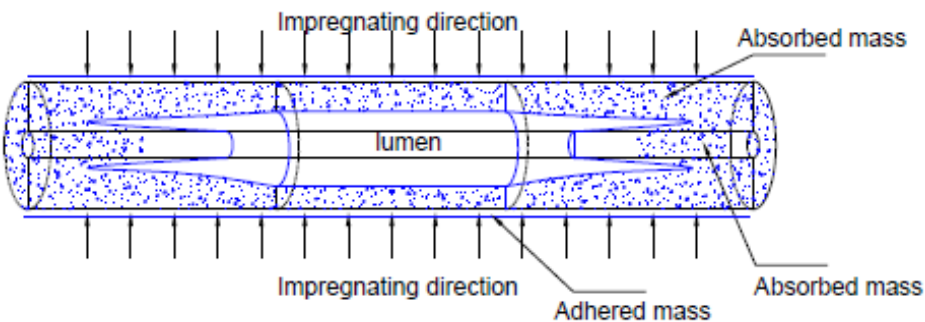
Porous fiber filament



Flax fiber in contact with the liquid resin

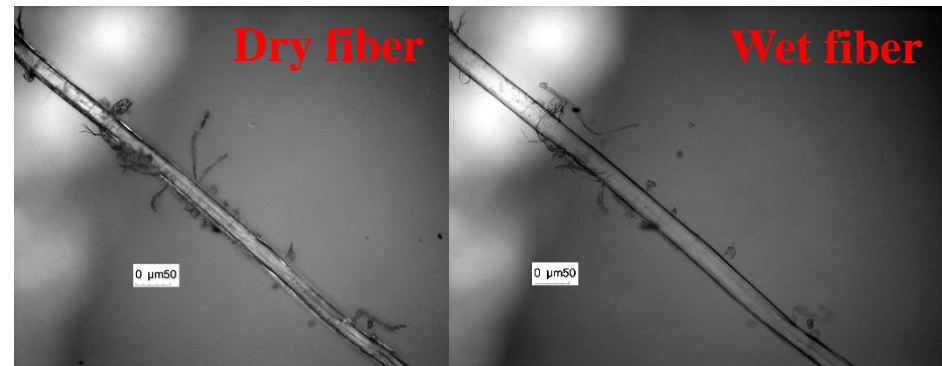
■ Liquid absorption

Liquid absorption into the fiber filament



■ Fiber swell

Increase of fiber diameter



Liquid Absorption & Fiber Swell

What influence on

the mechanical properties?

the resin **impregnation process?**

Impregnated Fiber Bundle Test (IFBT)

- Measurement of the mechanical properties of pure matrix and unidirectional composites
- Back-calculation of the mechanical properties of fibers

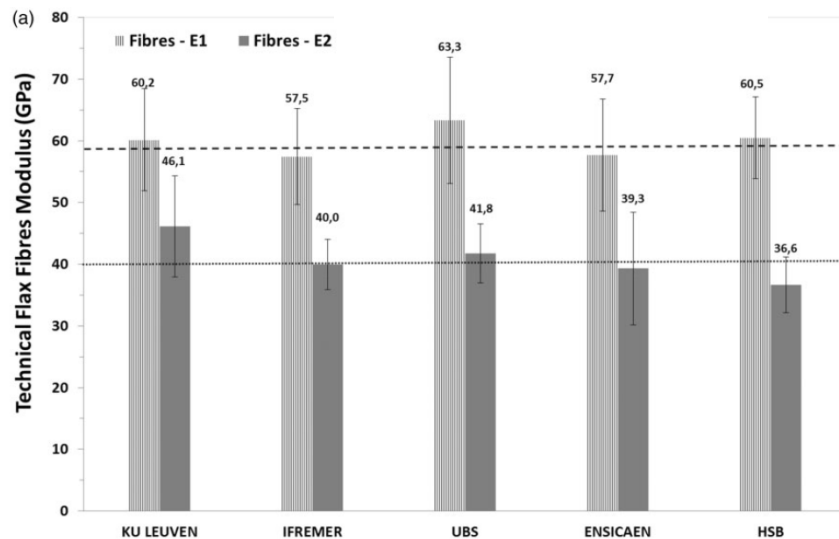
Statistical averaging

Benchmark tests by different labs

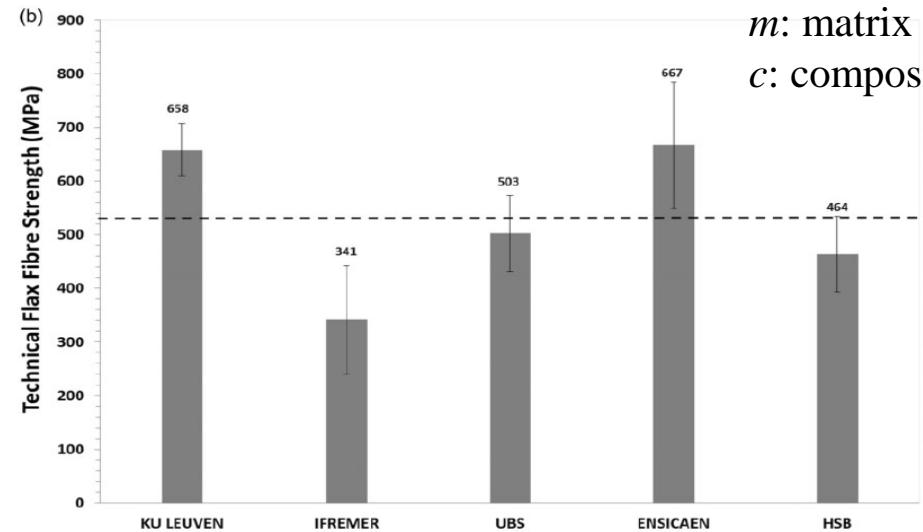
Bensadoun et al./JRPC/2017

Modulus $E_f = \frac{E_c - E_m \cdot (1 - V_f)}{V_f}$

Strength $\sigma_{u,f} = \frac{\sigma_c - \sigma'_m \cdot (1 - V_f)}{V_f}$ $\sigma'_m = E_m \times \varepsilon_c$
f: fiber
m: matrix
c: composite



Constant fiber modulus

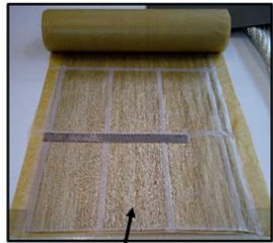


Variable fiber strength

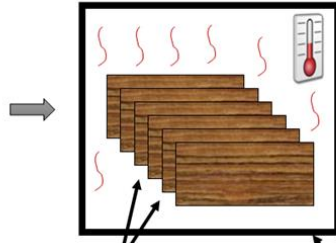
Influence of manufacturing conditions (void content, cure cycle) ?

UD Specimen Fabrication

1. Cutting flax fiber tape 2. Drying (60°C/14h)



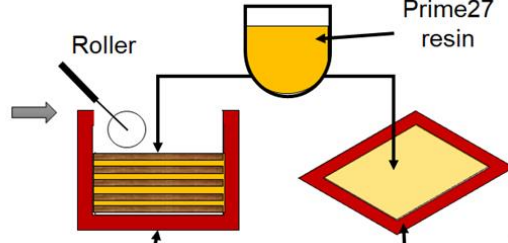
Flaxtape™110



UD flax fiber layers

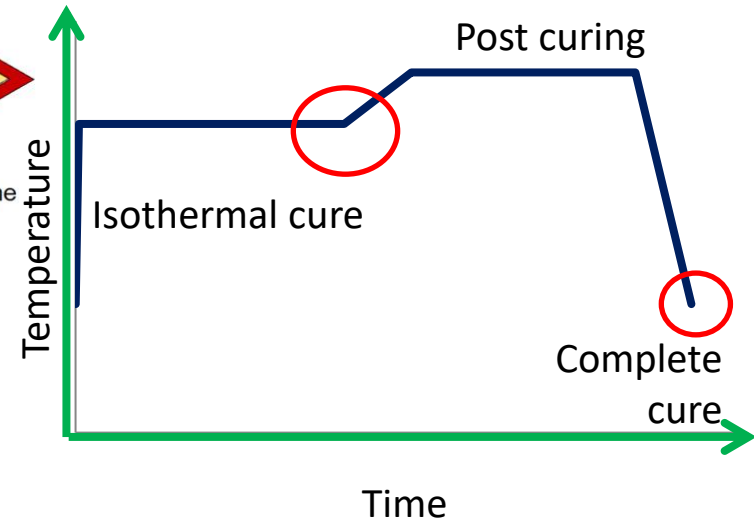
Oven

3. Hand layup (25°C/3 min)

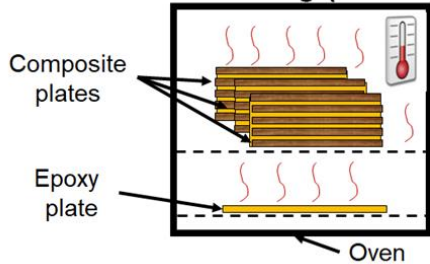


Pre-heated mould

Pre-heated frame

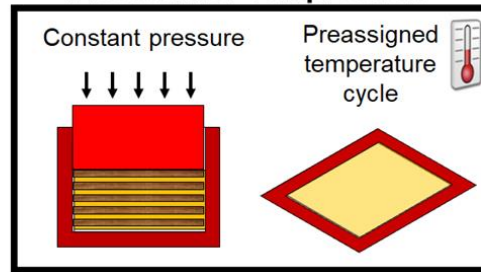


5. Post-curing (70°C/7h)



Oven

4. Isothermal compression



Different cure cycles, $T(t)$

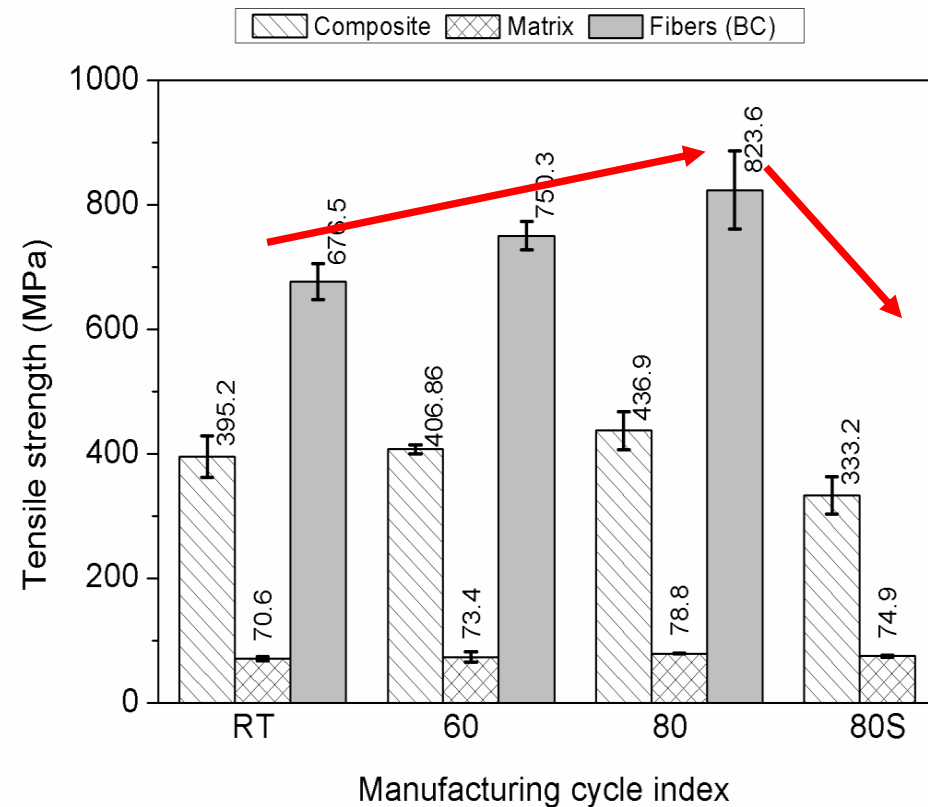
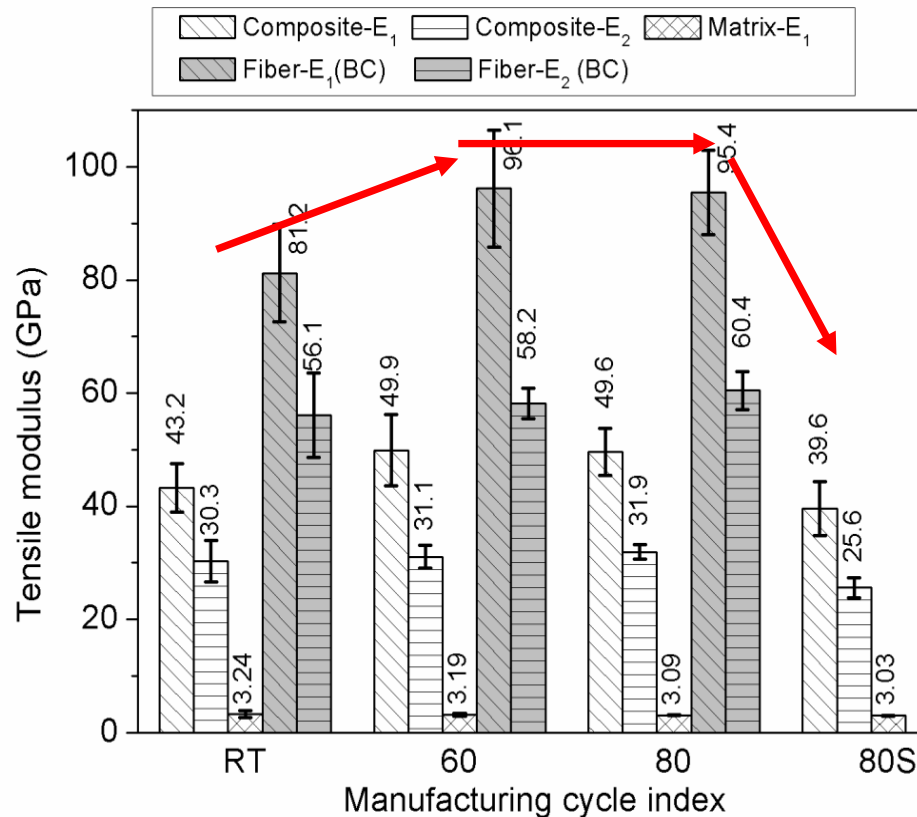
Hand lay-up to minimize the void content (<1% except 80S)

Cycle reference	Temperature(°C)
RT	25
60	60
80	80
80S	80

Temperature
Time

Modulus & Strength of Flax Fibers

- As the **temperature** increases, the fiber modulus/strength increases.
- At the same temperature, the strength is greater for a longer **duration** of cure (and impregnation).



Process optimization: Minimal temperature and duration

Resin Penetration into Flaw Fiber

Low temperature, Short time

Resin

Fiber

Impregnation

Fiber / matrix
wetting

Curing /
Cooling

Shrinkage of
matrix / fiber

μ



*Fiber/matrix
interface void*

High temperature, Long time

Resin

Fiber

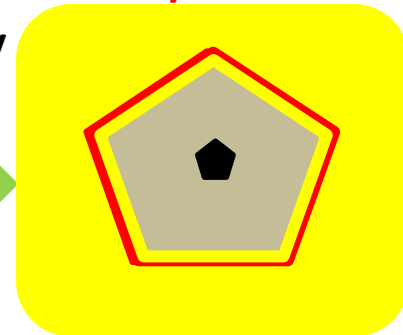
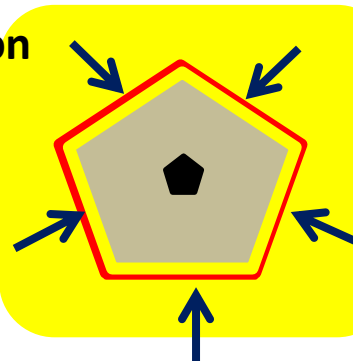
Impregnation

Resin penetration inside
the fiber cell walls

Mechanical interlocking
of fiber/matrix

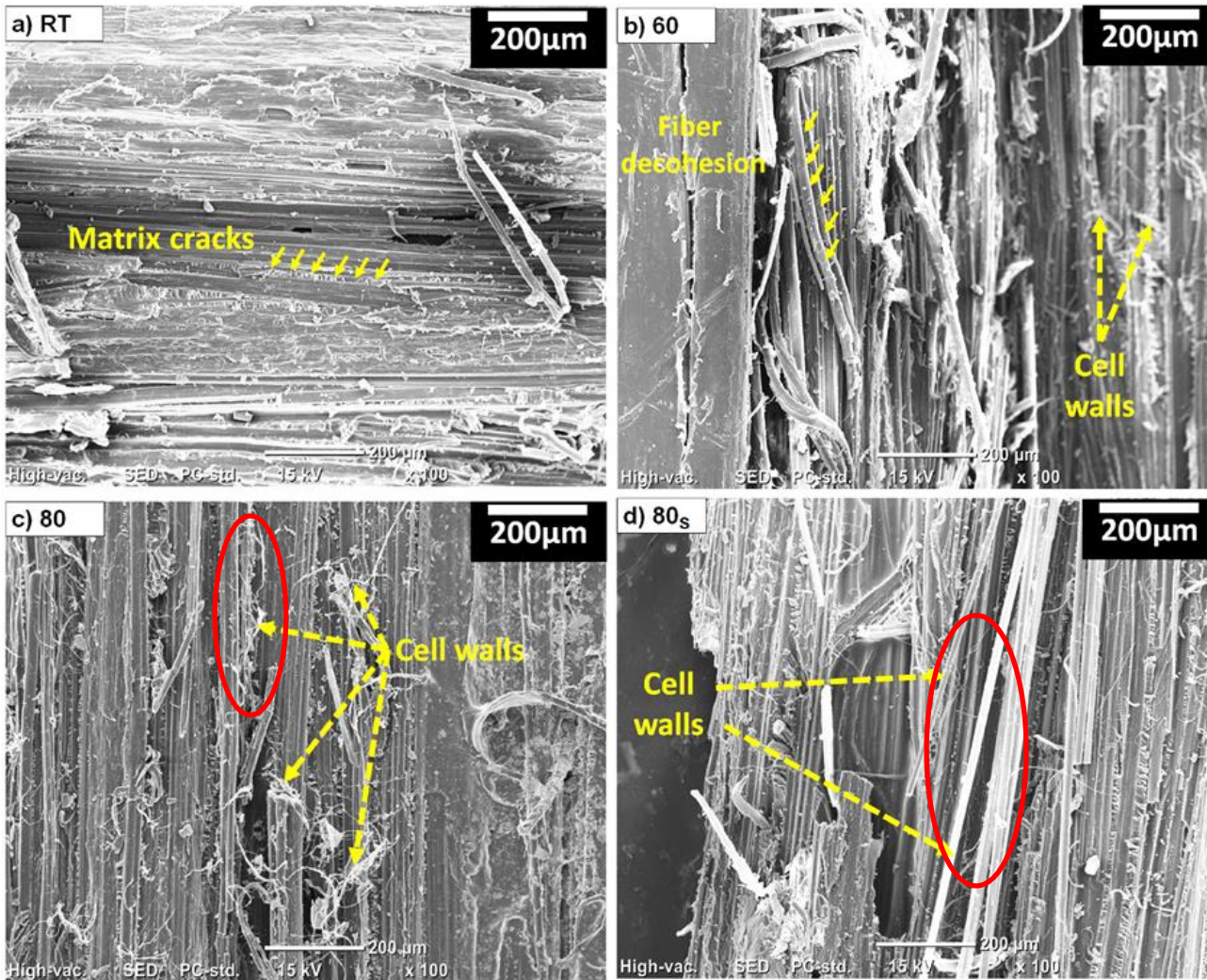
Curing /
Cooling

μ



Fractography

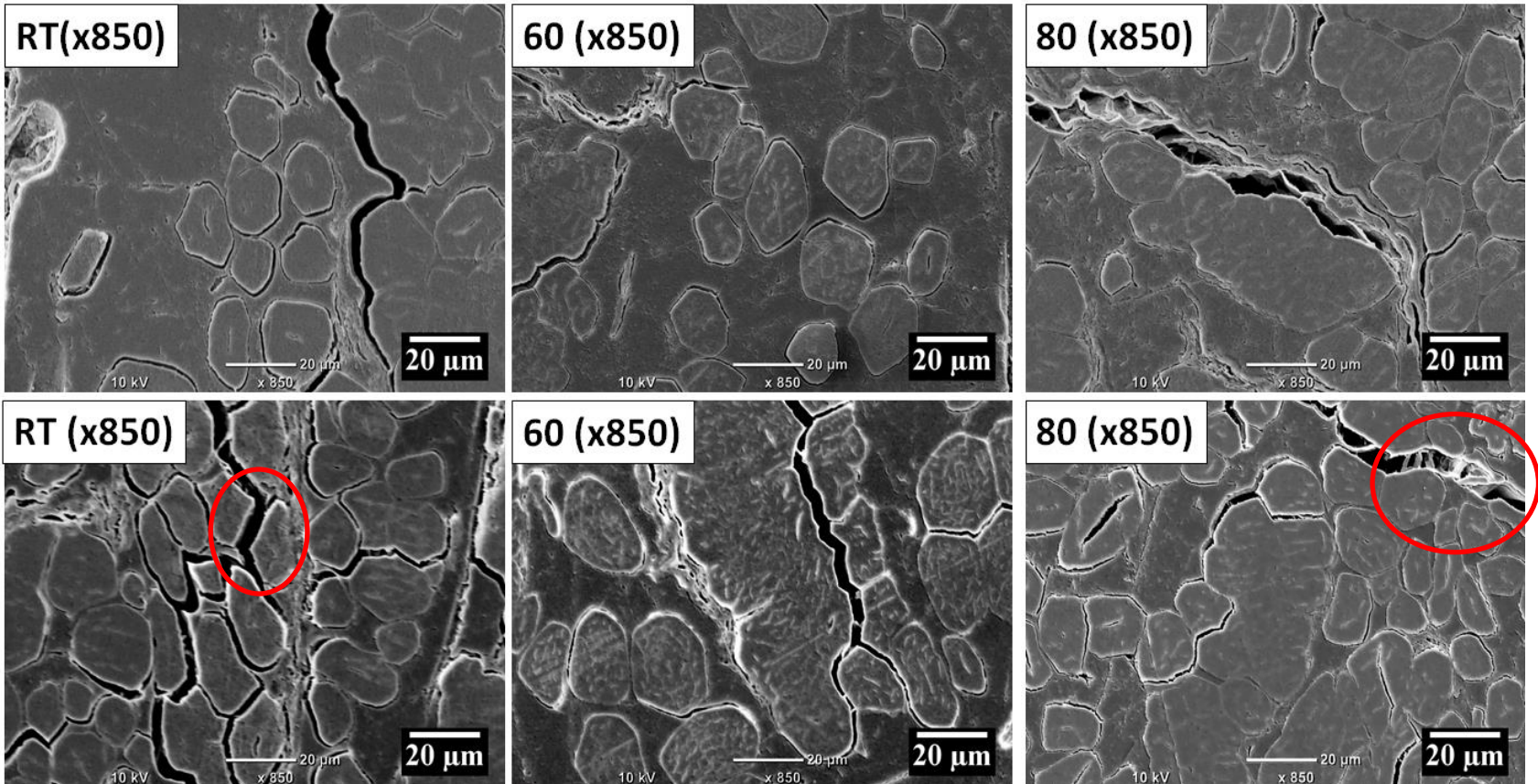
- At low temperature (and short duration), fiber/matrix separation at the interface.
- At high temperature (and long duration), fiber cell walls are torn off by the matrix.



SEM images of fractured surfaces of composite samples

Fractography

- At low temperature (and short duration), fiber/matrix separation at the interface.
- At high temperature (and long duration), fiber cell walls are torn off by the matrix.



SEM images showing the interfacial cohesion and decohesion for different cure cycles at the scale of individual fibers

Liquid Absorption & Fiber Swell

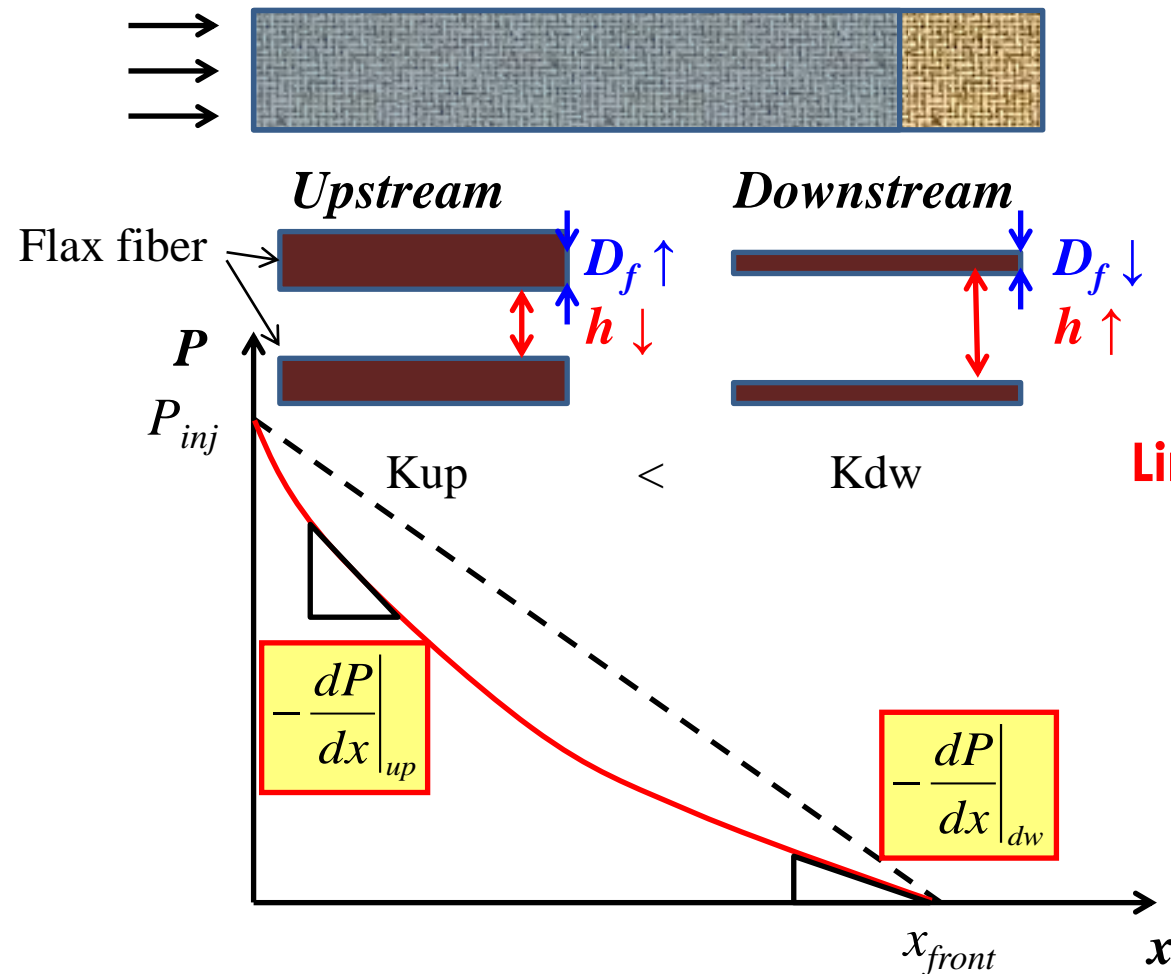
What influence on

the **mechanical properties?**

the resin impregnation process?

Unsaturated Flow in Flax Preform

Rectilinear injection under a constant inlet pressure



Transient flow

$P_I = \text{constant}$

Measure $L(t)$

$$\vec{u}_{pore} = -\frac{1}{1-V_f} \frac{\mathbf{K}}{\mu} \frac{dP}{dx} \Big|_{x=L}$$

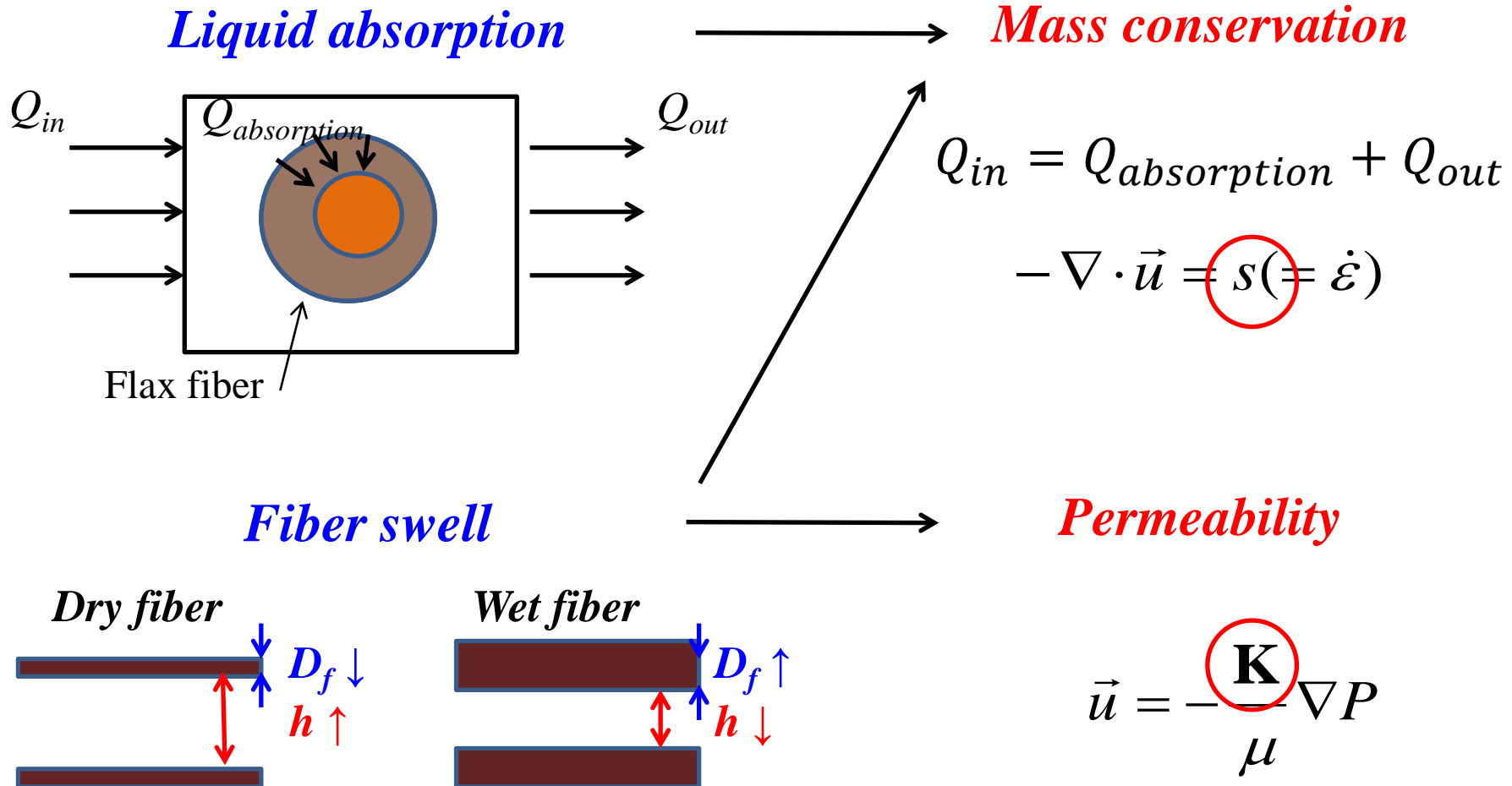
Linear pressure distribution

$$-\frac{dP}{dx} = \frac{P_1 - P_2}{L}$$

$$\frac{dL(t)}{dt} = \frac{1}{1-V_f} \frac{\mathbf{K}}{\mu} \frac{P_1}{L(t)}$$

$$\mathbf{K}_{unsat} = \frac{(1-V_f)\mu L^2}{2P_1 t}$$

Modeling Approach



Fiber Swell

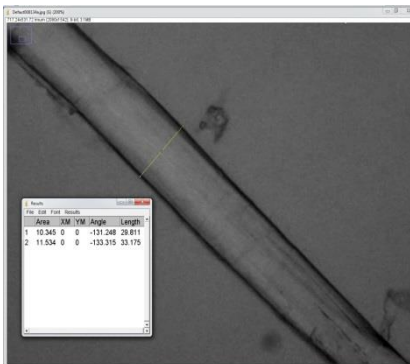
Optical observation of the fiber diameter change immersed in test liquid

The flax fiber cross-section is not circular but polygonal; the equivalent diameter is considered.

Dry fiber diameter: $D_{f,o}$

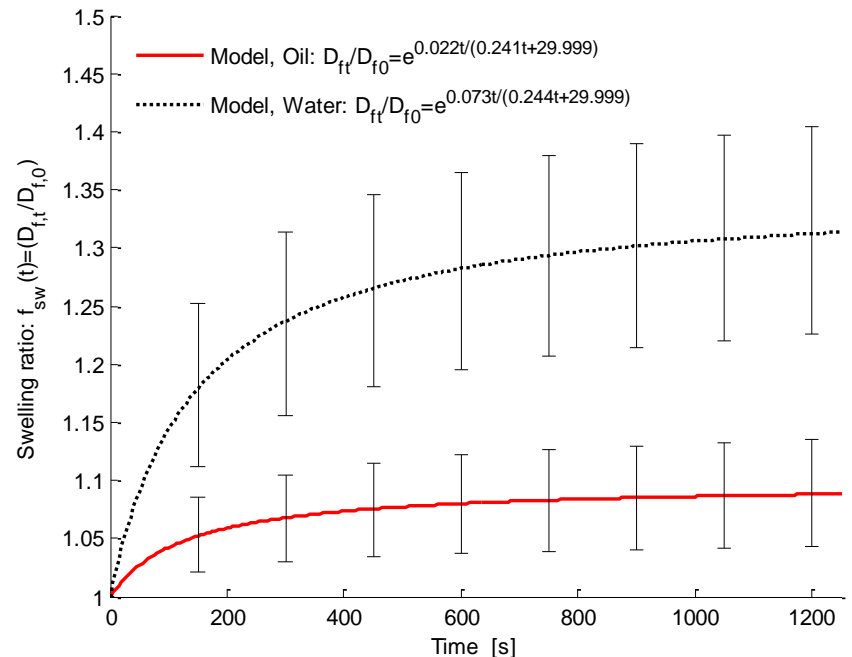


Wet fiber diameter: $D_{f,t}(t)$



Fiber swell ratio

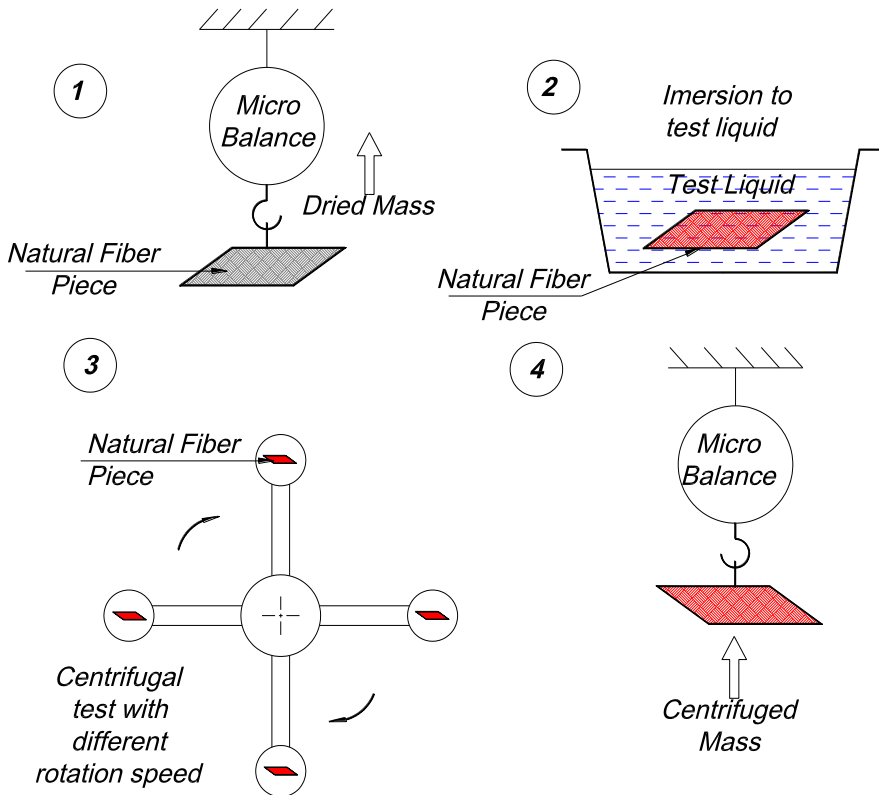
$$f_{sw}(t) = \frac{D_{wet\ fiber}(t)}{D_{dry\ fiber}} = \frac{D_{f,t}(t)}{D_{f,o}}$$



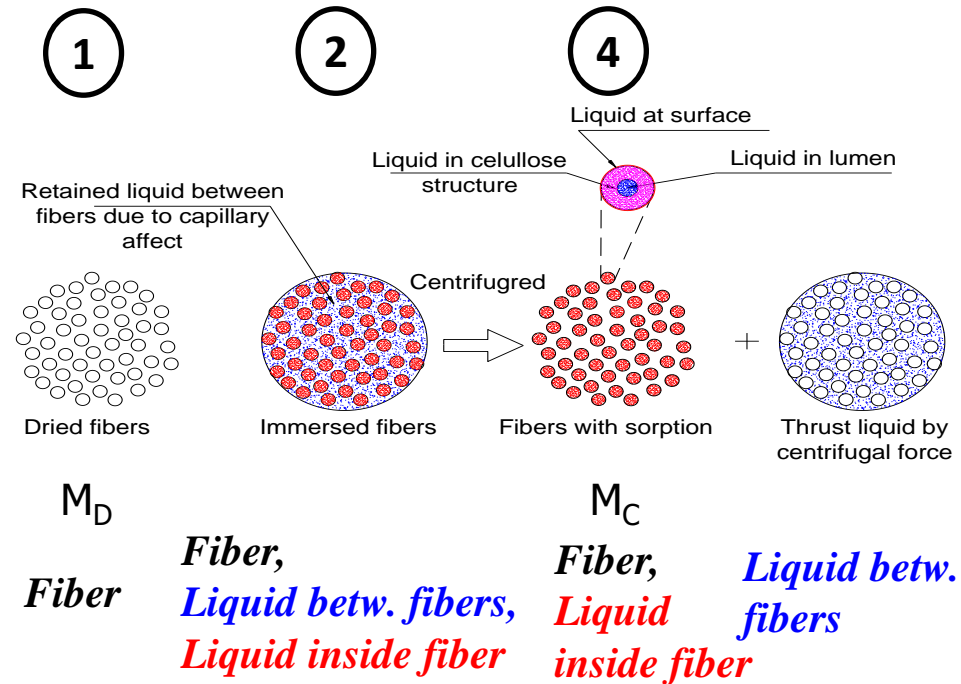
Liquid Absorption

Comparing the mass of dry and wet bundle samples

Experimental procedure



Mass change during centrifugal test

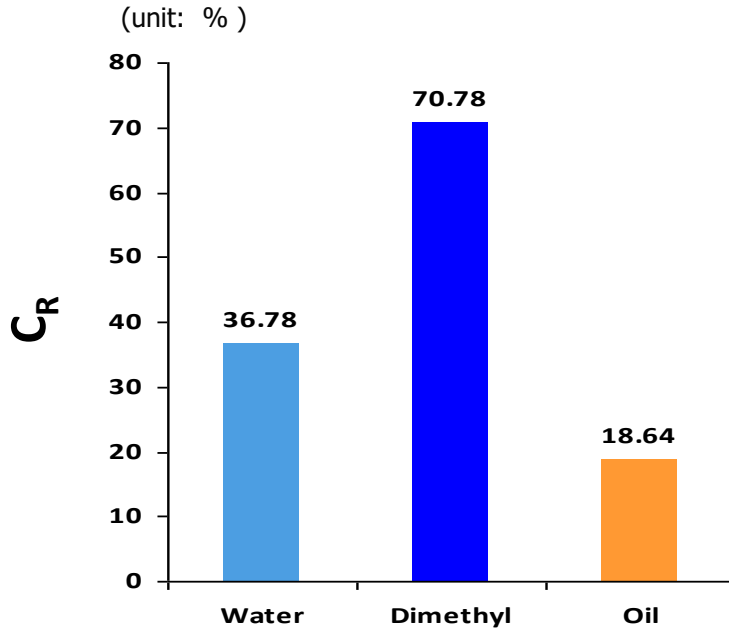


$$C_R = 100 \times \frac{M_a}{M_D} = 100 \times \frac{(M_C - M_D)}{M_D}$$

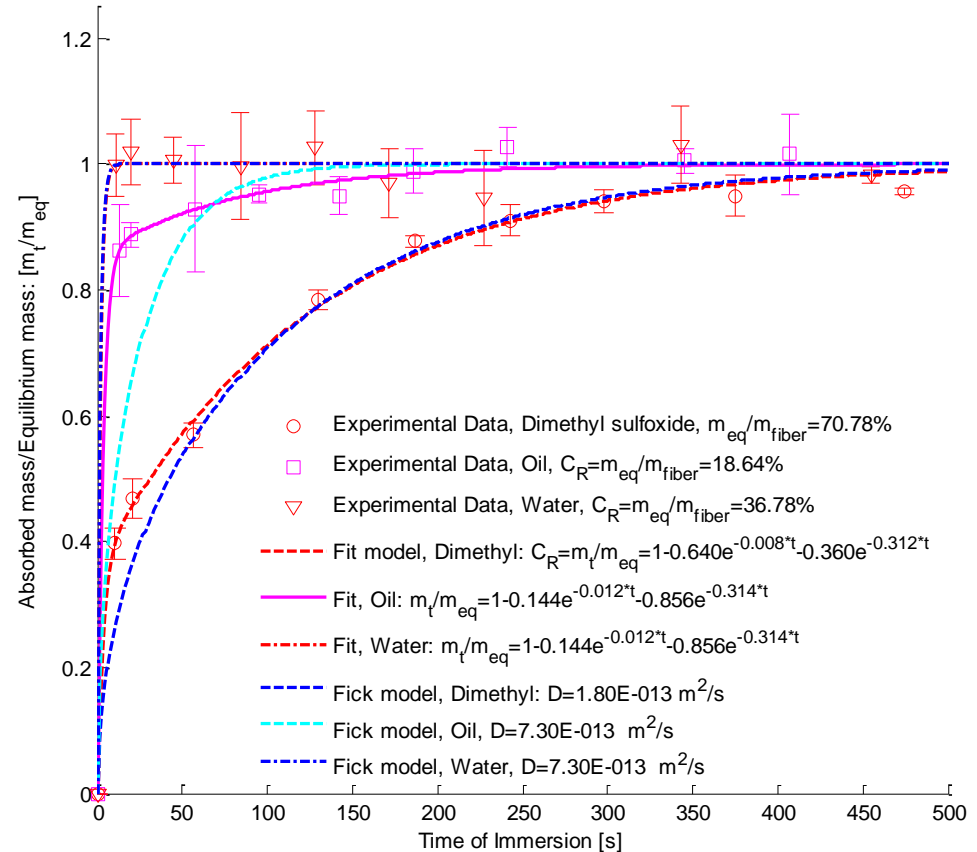
Liquid Absorption

Maximum liquid retention rate

$$C_R = 100 \times \frac{M_a}{M_D} = 100 \times \frac{(M_C - M_D)}{M_D}$$



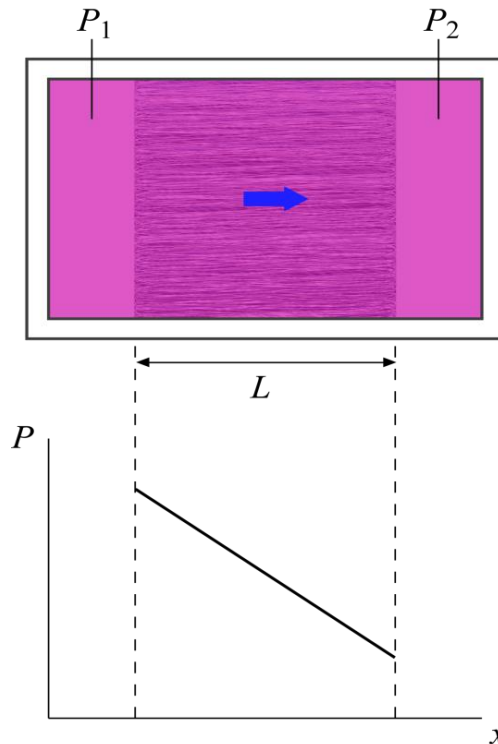
Liquid absorption mass change with time



Permeability Measurement

■ **Unsaturated permeability: time-dependent fiber swell, non-uniform permeability**

■ **Saturated permeability (K_{sat})**



Steady flow at maximum fiber swell (uniform in the preform)

$$\vec{u}_{Darcy} = -\frac{\mathbf{K}}{\mu} \frac{dP}{dx}$$

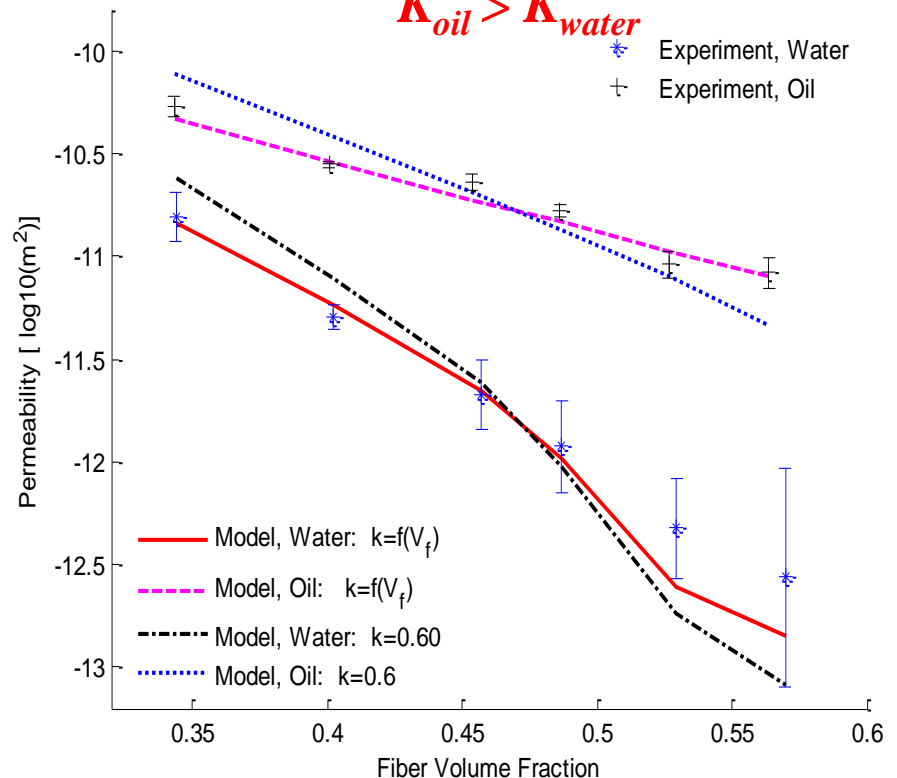
$$\frac{Q}{A} = \frac{\mathbf{K}}{\mu} \frac{P_1 - P_2}{L}$$

$$\mathbf{K}_{sat} = \frac{Q\mu L}{A(P_1 - P_2)}$$

Two test liquids with different fiber swell ratios

$$f_{sw,oil} < f_{sw,water}$$

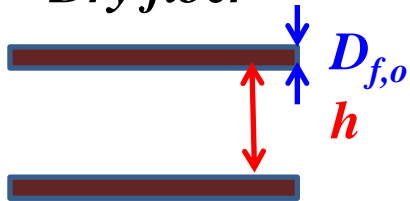
$$K_{oil} > K_{water}$$



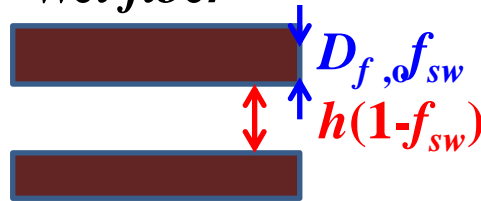
Permeability Model

■ $K(V_{f,eff}=f_{sw}^2 V_f)$

Dry fiber



Wet fiber

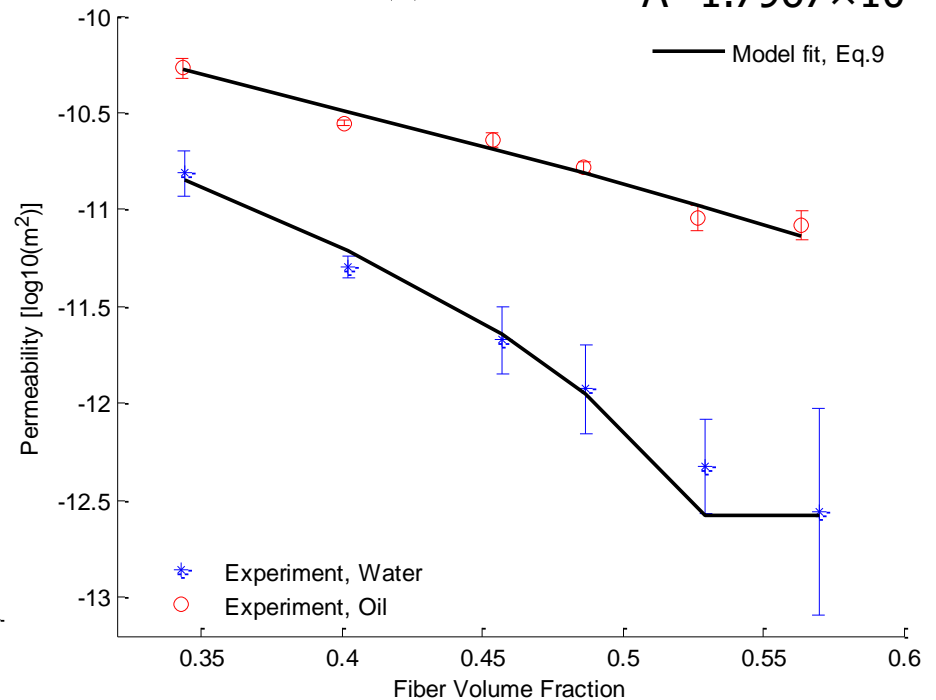
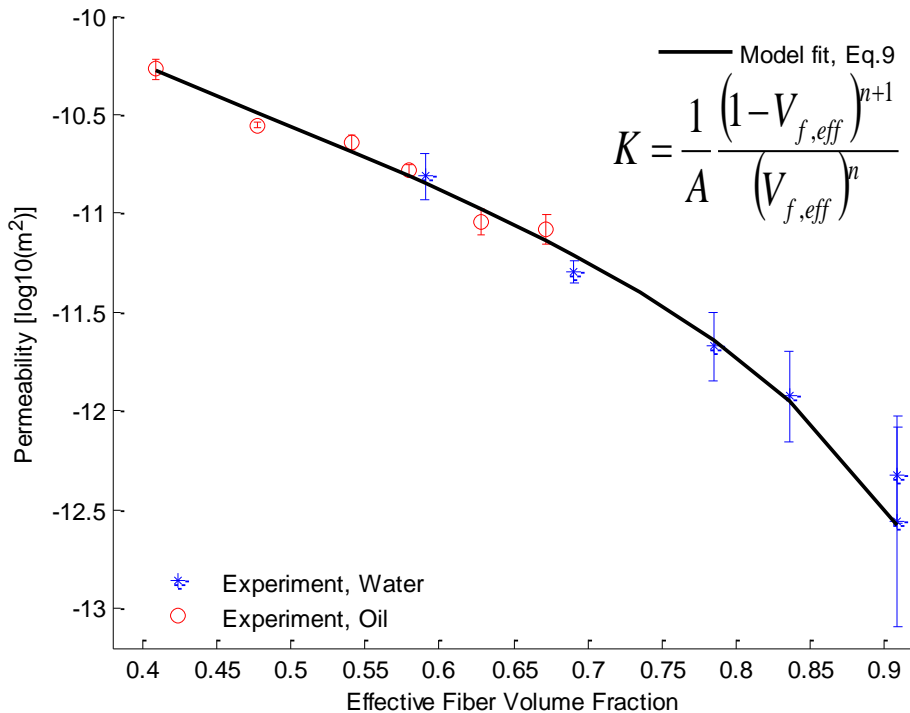


■ $K(V_{f,dry}, f_{sw})$

$$K = \frac{1}{A} \frac{(1 - f_{sw}^2 V_f)^{n+1}}{(f_{sw}^2 V_f)^n}$$

$$f_{sw} = f(t)$$

$n=1.2855$
 $A=1.7967 \times 10^{10}$



Multi-Scale Flow in Flax Preform

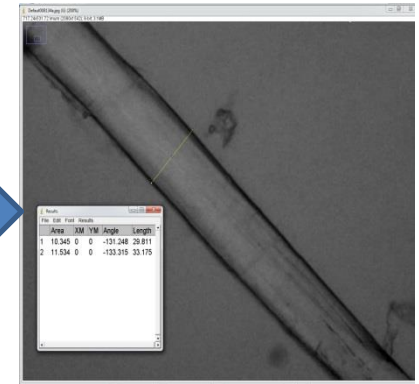
Fabric ($D_p: 0.1\sim 1\text{mm}$)



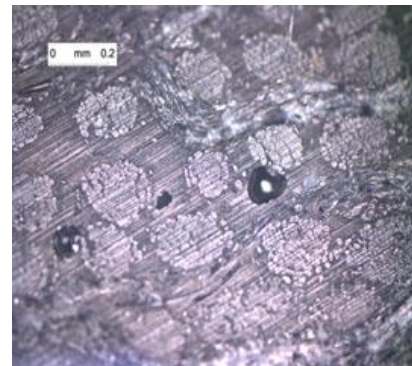
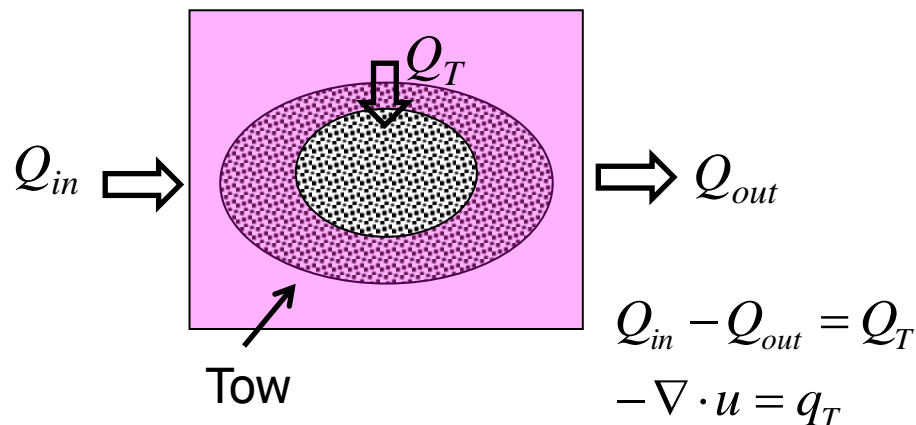
Yarn ($D_p: 1\sim 10\mu\text{m}$)



Fiber filament ($D_p: < 1\mu\text{m}$)



Unsaturated flow effect from void inside the tow is **insignificant**.



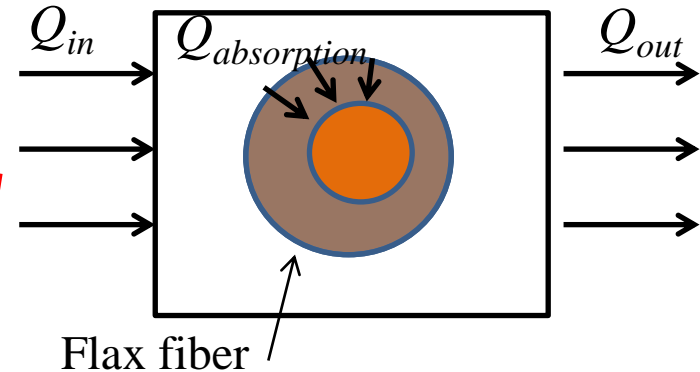
- ✓ Yarn diameter ~ 0.2 mm
- ✓ Contact angle $\ll 90^\circ$
- ✓ No intra-yarn void

Mass Conservation Equation

Liquid absorption: Mass sink

$$Q_{in} - Q_{out} = Q_{absorption}$$

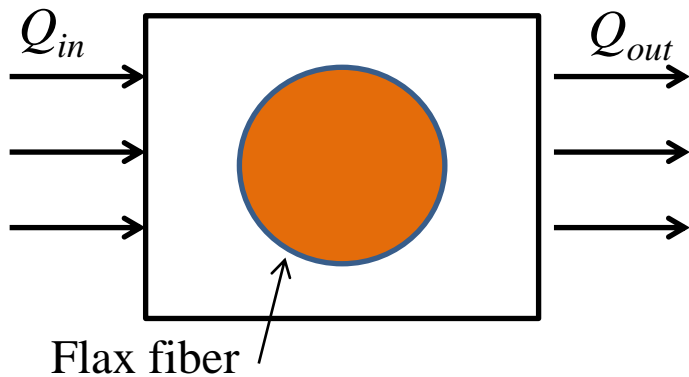
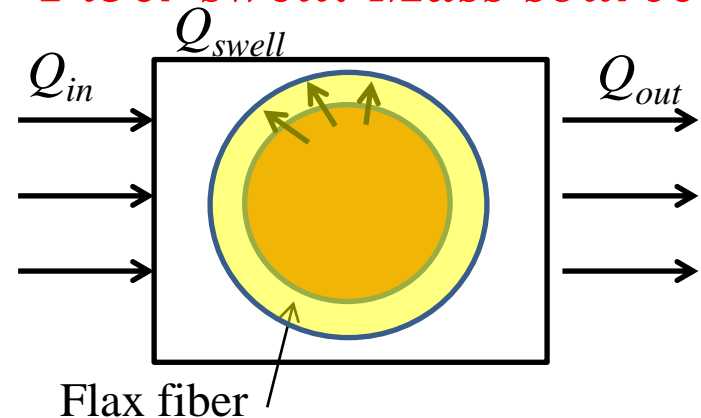
$$-\nabla \cdot \vec{u} = s_{sink}$$



Fiber swell: Mass source

$$Q_{in} - Q_{out} = -Q_{swell}$$

$$-\nabla \cdot \vec{u} = -s_{source}$$



Mass Sink & Source

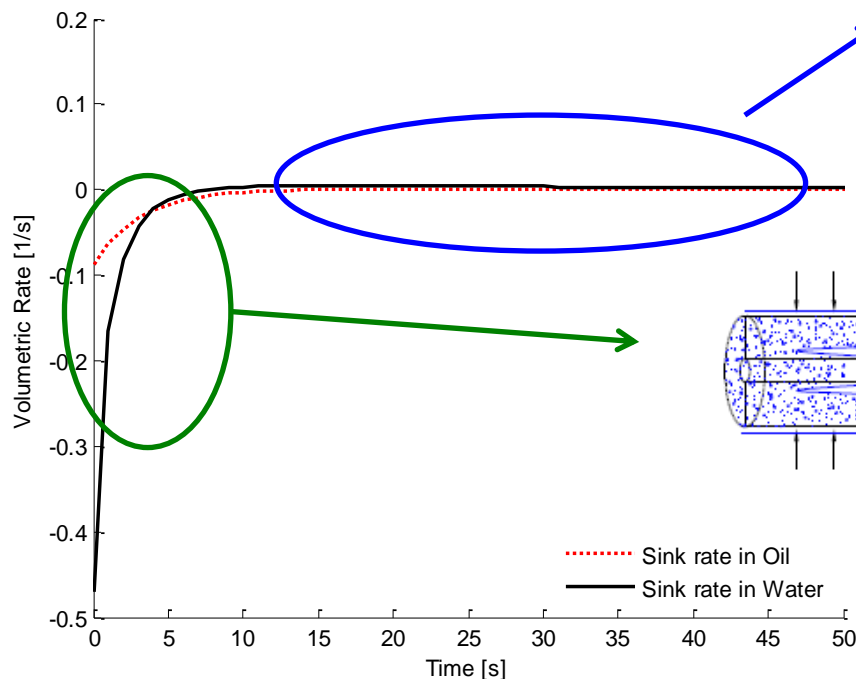
$$-\nabla \cdot \vec{u} = s_{sink} - s_{source} = s$$

$$-\nabla \cdot \left(-\frac{K(x,t)}{\mu} \nabla P \right) = s(x,t)$$

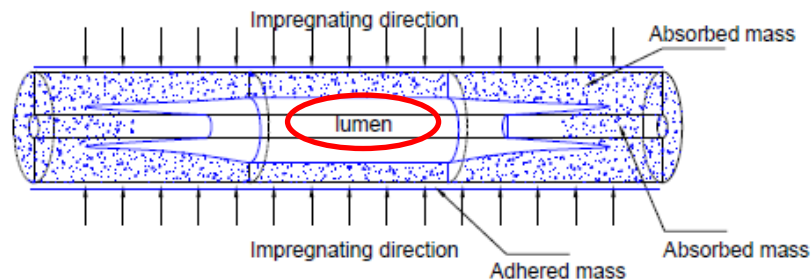
Sink by absorption & Source by swell

$$\begin{aligned} K(t_{immers}) &= K(x, t) \\ s(t_{immers}) &= s(x, t) \end{aligned} \quad s_{micro}(t) = \frac{V_{f,0}}{1-V_{f,0}} \left(\frac{\partial f_{sw}^2(t)}{\partial t} - \frac{C_R}{\rho_l} \frac{\partial f_{so}(t)}{\partial t} \right)$$

Mass sink and source terms are not cancelled out!



Once the lumen is filled with the liquid, fiber swells at the same rate of liquid absorption: Sink = Source



Liquid fills the lumen without significant fiber swell: Sink > Source

Comparison of Different Models

Models in the literature

- Model 1

$$-\nabla \cdot \left(-\frac{K}{\mu} \nabla P \right) = 0$$

$K = \text{const.}$

- Model 2

$$-\nabla \cdot \left(-\frac{K(x,t)}{\mu} \nabla P \right) = 0$$

$K(x,t)$: non-uniform in the preform

Current model

- Model 3

$$-\nabla \cdot \left(-\frac{K(x,t)}{\mu} \nabla P \right) = s(x,t)$$

Experimental measurement

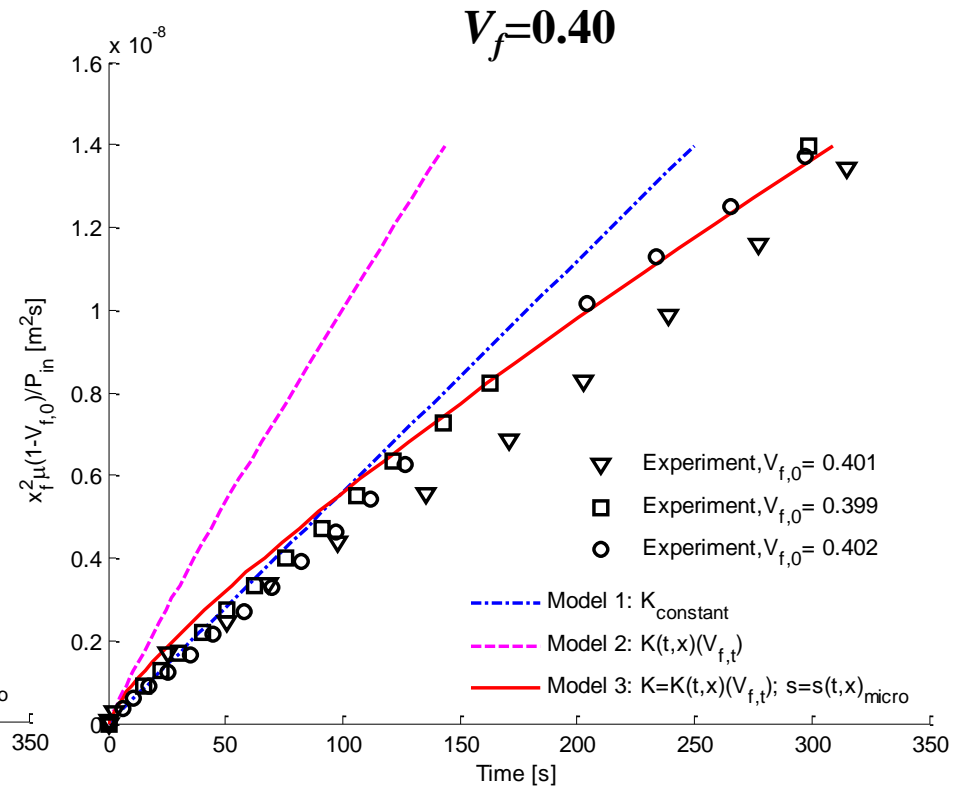
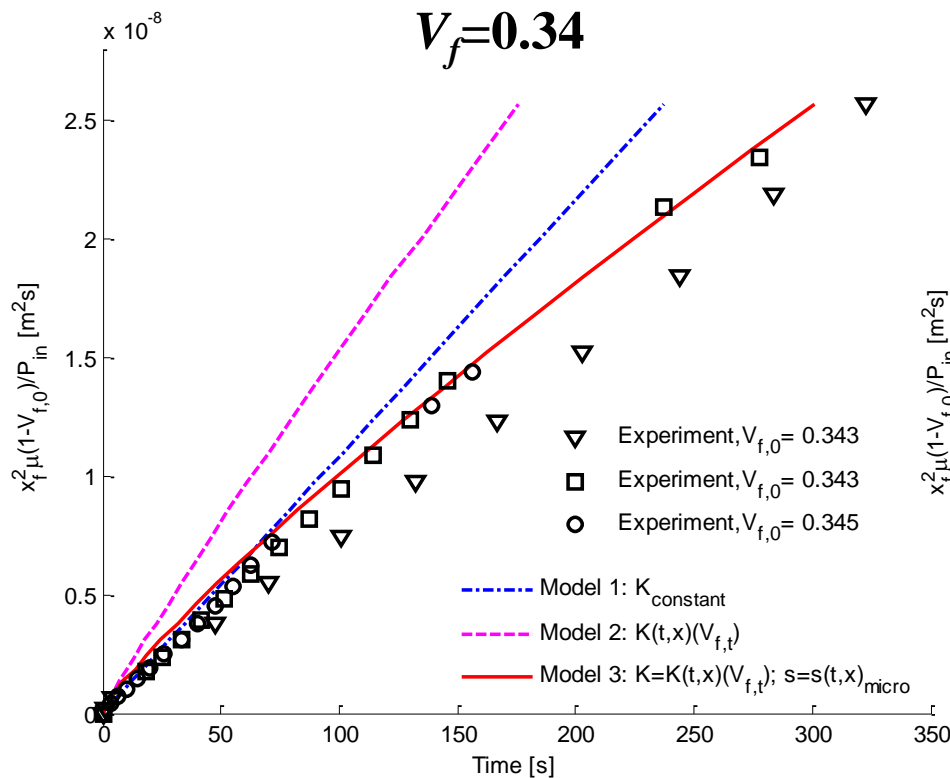
- ✓ Twill weave flax fabric + Engine oil
- ✓ 6 fiber volume fraction values / 3 measurements per condition

Experimental & Modeling Results

Flow front position square vs. time / Low fiber volume fraction

- ✓ Model 3 ($K(x,t)$ with sink) shows the best agreement.
- ✓ Model 1 ($K=\text{const.}$) also works pretty well.

\cdots $K=\text{const.}$
 $---$ $K(x,t)$
 $---$ $K(x,t)$ & sink

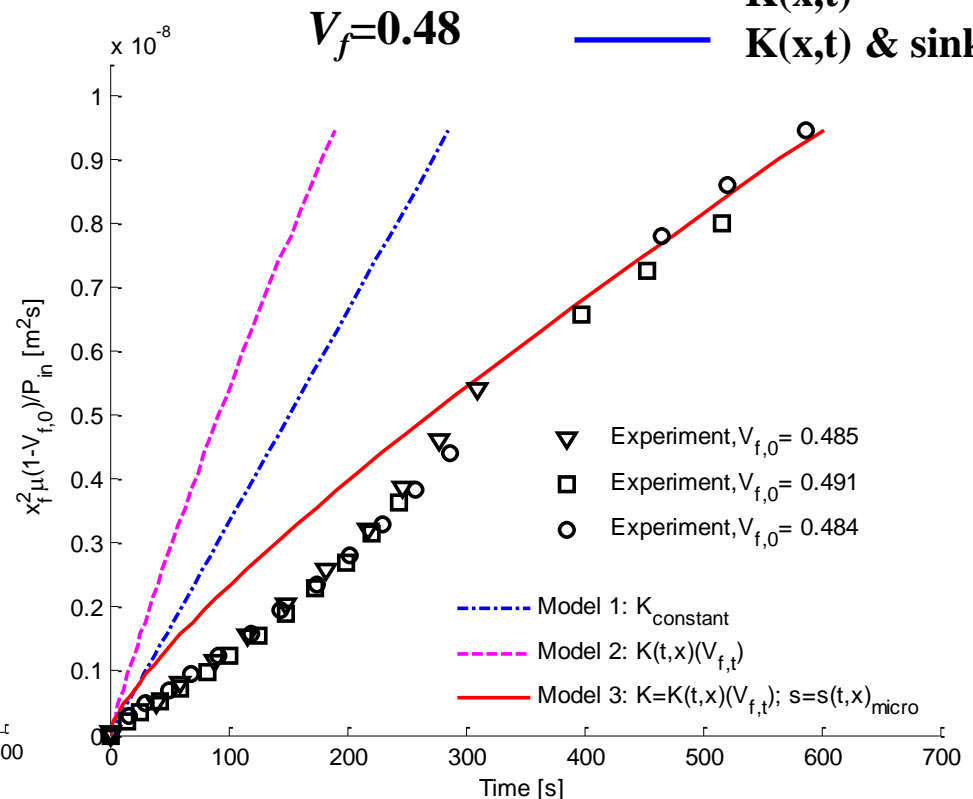
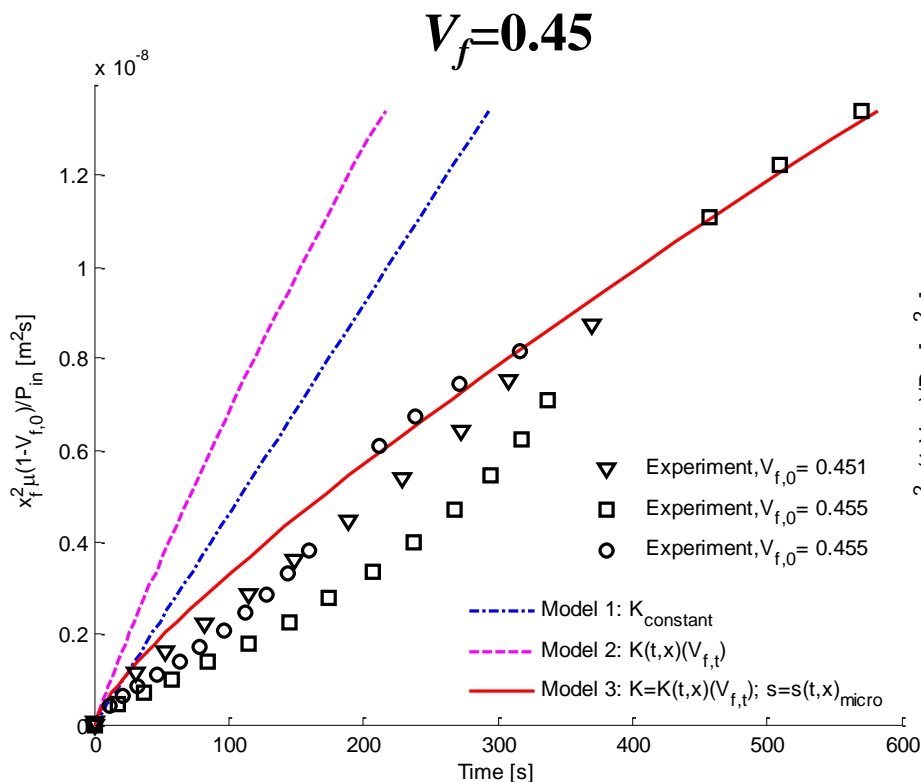


Experimental & Modeling Results

Flow front position square vs. time / Intermediate fiber volume fraction

- ✓ Model 1 ($K=\text{const.}$) and Model 2 ($K(x,t)$) overestimates the experimental data.
- ✓ As V_f increases, mass sink effect becomes important.

- · - · - $K=\text{const.}$
 - - - $K(x,t)$
 — $K(x,t)$ & sink

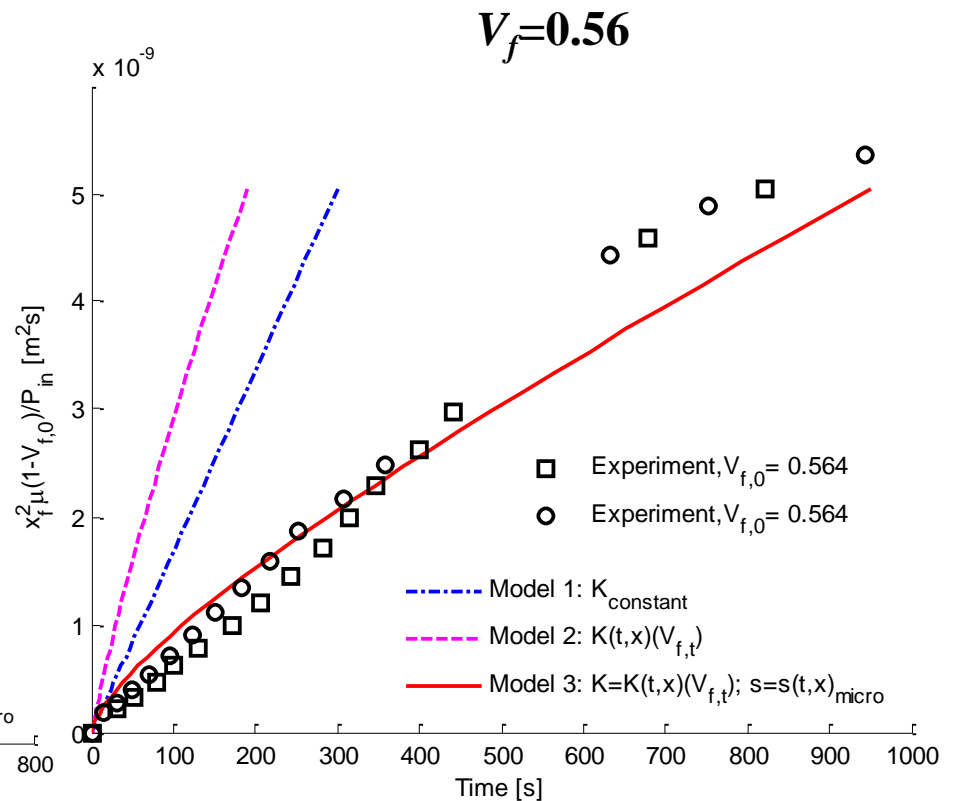
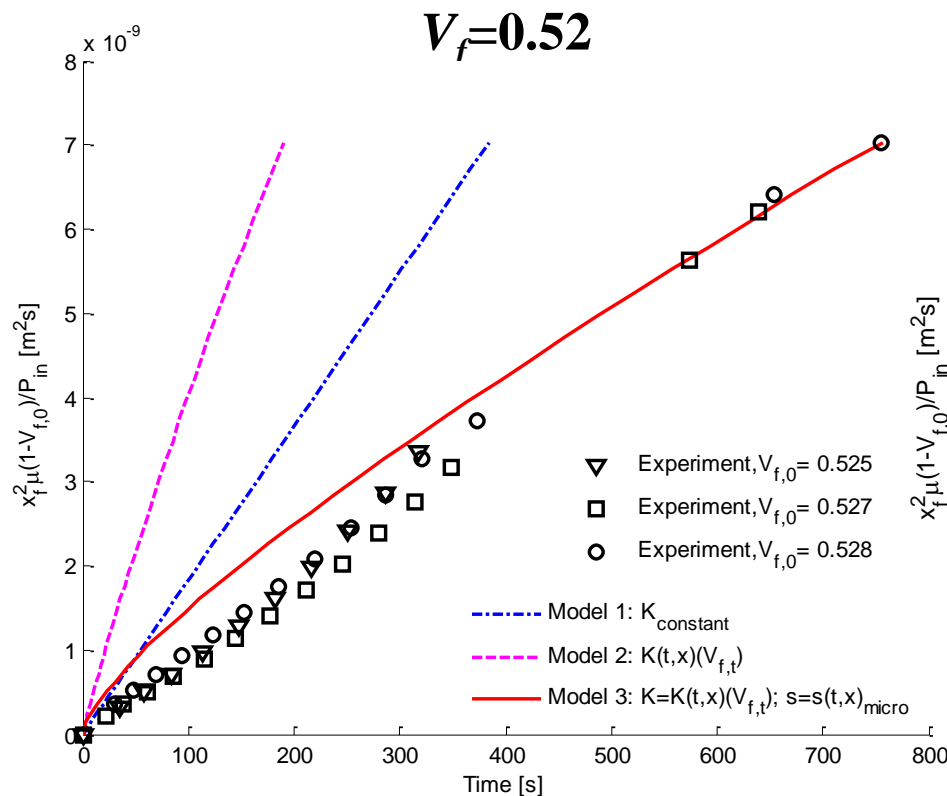


Experimental & Modeling Results

Flow front position square vs. time / High fiber volume fraction

✓ At high V_f , mass sink effect that delays the flow front advancement is remarkable.

$\text{---} \cdot \text{---}$ $K=\text{const.}$
 --- $K(x,t)$
 --- $K(x,t) \text{ \& sink}$



Conclusions

- Flax fiber takes up the liquid during the resin impregnation process and the fiber cross-section (or equivalent diameter) increases with time.
- Fiber swell phenomenon changes the permeability.
- Fiber swell and liquid absorption play the role of mass sink/source affecting the flow front advancement.
- The influence of the fiber swell and liquid absorption on the resin flow becomes more significant as the fiber volume fraction and the preform size increase.

Further Reading

- **C.H. Park**, “Chapter 15. Numerical simulation of flow processes in composites manufacturing,” *Advances in Composites Manufacturing and Process Design*, Edited by P. Boisse, ISBN 978-1-78242-307-2, pp. 317-348, July 2015, Woodhead Publishing.
- V.H. Nguyen, M. Lagardère, **C.H. Park**, S. Panier, “Permeability of natural fiber reinforcement for liquid composite molding processes,” *Journal of Materials Science*, Vol. 49(18), pp. 6449-6458, 2014, Springer.
- V.H. Nguyen, M. Deléglise-Lagardère, **C.H. Park**, “Modeling of resin flow in natural fiber reinforcement for liquid composite molding processes,” *Composites Science and Technology*, Vol. 113, pp. 38-45, 2015, Elsevier.
- G.A. Testoni, S. Kim, A. Pisupati, **C.H. Park**, “Modeling of the capillary wicking of flax fibers by considering the effects of fiber swelling and liquid absorption,” *Journal of Colloid and Interface Science*, Vol. 525, pp. 166-176, 2018.